Transactions of Karelian Research Centre
of Russian Academy of Sciences
December, 2015
DOI: 10.17076/geo265

Труды Карельского научного центра РАН
2015, декабрь

УДК 552.16:552.18 (470.2+48) +551.71/.72+553.411

SCHEME OF MINERAL FACIES OF METAMORPHIC ROCKS AND ITS APPLICATION TO THE FENNOSCANDIAN SHIELD WITH REPRESENTATIVE SITES OF OROGENIC GOLD MINERALIZATION

S. A. Bushmin, V. A. Glebovitsky

Institute of Precambrian Geology and Geochronology RAS

Our recent studies of metamorphism within the Fennoscandian (or Baltic) Shield area with representative sites of orogenic gold mineralization based on the scheme of mineral facies of metamorphic rocks introduced earlier inspired thorough revision of that scheme. The proposed scheme retains the commonly adopted nomenclature (prehnite-pumpellyite, greenschist, amphibolite, granulite, blueschist and eclogite facies) and is based on thermodynamic calculations and published empirical and experimental data on mineral equilibria in metapelitic and metamafic rocks.
We present two simplified maps of Archean and Proterozoic metamorphism, that offer good examples of the application of this improved scheme of metamorphic facies. The maps specify the prevailing metamorphic conditions and their relevant tectonic settings. Gold mineralization of economic interest is spatially associated with low-temperature low-pressure metamorphic terrains metamorphosed at the greenschist to low amphibolite facies of the andalusite-sillimanite facial series.

K e y w o r d s: metamorphic facies; metamorphism; mineral reaction; mineral paragenesis; P-T conditions; T/P gradient; orogenic gold; shear zone; accretionary orogen.

С. А. Бушмин, В. А. Глебовицкий. СХЕМА МИНЕРАЛЬНЫХ ФАЦИЙ МЕТАМОРФИЧЕСКИХ ПОРОД И ЕЕ ПРИМЕНЕНИЕ К ТЕРРИТОРИИ ФЕННОСКАНДИНАВСКОГО ЩИТА С ПРОЯВЛЕНИЯМИ ЗОЛОТОРУДНОЙ МИНЕРАЛИЗАЦИИ ОРОГЕННОГО ТИПА

В процессе исследования особенностей метаморфизма в районах Фенноскандинавского (или Балтийского) щита с проявлениями золоторудной минерализации орогенного типа частично изменена ранее предложенная схема минеральных фаций метаморфических пород. Предлагаемая новая схема, сохраняющая традиционные названия фаций (пренит-пумпеллиитовая, зеленосланцевая, амфиболитовая, гранулитовая, голубых сланцев, эклогитовая), основана на оригинальных термодинамических расчетах и опубликованных расчетных и экспериментальных данных по минеральным равновесиям в метапелитах и метабазитах и учитывает новые данные по метаморфизму изученной территории.
Статья сопровождается двумя упрощенными картами метаморфизма архейского и протерозойского возраста в качестве примера применения схемы метаморфических фаций при исследовании P-T условий метаморфизма и особенностей их пространственной локализации. Показано, что все промышленные проявления золотой минерализации орогенного типа расположены в зонах LT-LP метаморфизма от зеленосланцевой до низкотемпературной амфиболитовой фаций And-Sil фациальной серии.

Ключевые слова: метаморфическая фация; метаморфизм; минеральная реакция; минеральный парагенезис; P-T условия; T/P градиент; орогенное золото; сдвиговая зона; аккреционный ороген.

1. Introduction

Our study of metamorphism was focused on the Fennoscandian (or Baltic) Shield area with representative sites of orogenic gold mineralization (the term is according to [Groves et al., 1998]) and encompasses parts of the major tectonic units of the Fennoscandian Shield (Karelian craton, Svecofennian accretionary orogen, Belomorian-Lapland collision orogen). In the course of this study the scheme of mineral facies of metamorphic rocks introduced earlier by Bushmin and Glebovitsky [2008] was thoroughly revised. The paper is accompanied by two simplified maps of metamorphism of Archean and Proterozoic age as examples illustrating the application of the improved scheme of metamorphic facies to investigation of metamorphism. The abbreviations of minerals and other symbols used in this paper are listed in Table 1.

According to Eskola's facies concept [Eskola, 1920], the mineral composition of metamorphic rocks is a reflection of the external P-T conditions of metamorphism and the bulk rock chemistry. Thus, the variations in the mineral paragenesis at an unchanging bulk rock composition reflect changes in the P-T conditions. The term «mineral paragenesis» denotes sets of coeval equilibrium minerals. Mineral parageneses provide information on the physical-chemical conditions of metamorphism. Thus, metamorphic mineral facies/subfacies (or just metamorphic facies/subfacies) define the P-T regions in which certain groups of metamorphic rocks are made up of certain mineral parageneses.

So far, various schemes of metamorphic mineral facies have been developed in P-T space [e. g. Fyfe, 1962; Dobretsov et al., 1970, 1972, 1974; Glebovitsky, 1973; Winkler, 1976; Glebovitsky, 1977; Korikovsky, 1979; Spear, 1993; Bushmin, Glebovitsky, 2008]. Mineral facies define mineral parageneses for various rock types and are based on petrogenetic grids that always pertain to certain chemical systems, e. g. KFMASH, etc. The main purpose of the schemes is to specify the relative position and PT-boundaries of mineral facies and subfacies. The areas of metamorphic rocks corresponding to certain mineral facies and subfacies shown in metamorphic maps will demonstrate the P-T conditions of metamorphism and the spatial distribution of these parameters.

The facies and subfacies are determined first of all using the compositions of metapelites and metabasites. Metapelites rich in potassium are most susceptible to variations in P-T conditions and are thus the potential source of the most detailed information about the conditions of metamorphism. Most researchers [e. g. Dobretsov et al., 1970; Glebovitsky, 1977; Spear, 1993; Berman et al., 2000; Bucher, Frey, 2002; Bushmin, Glebovitsky, 2008] consider similar mineral reactions as facies boundaries in metapelitic and metabasic rocks. These are so-called «key mineral reactions». The reasons for minor differences in positions of these reactions in P-T space are inconsistencies in the thermodynamic databases used in the calculations, variations in the water activity in the fluid, and the results of experiments.

The following mineral reactions are most commonly recognized as the temperature boundaries of metamorphic facies and subfacies in metapelites:

- kaolinite decomposition (a typical supergene mineral) with pyrophyllite formation
- first appearance of muscovite and chlorite, and then biotite and garnet (almandine)
- chloritoid decomposition and staurolite appearance
- staurolite decomposition
- muscovite decomposition with the formation of K-feldspar in parageneses with aluminum silicates (andalusite, sillimanite, kyanite); and the simultaneous appearance of migmatites
- biotite decomposition and orthopyroxene appearance, first in parageneses with K-feldspar and then with K-feldspar+cordierite
- appearance of the spinel+quartz and sapphirine+quartz parageneses.

The equilibria of Al_2SiO_5 polymorphs (kyanite, andalusite, and sillimanite) with the triple point at P = 3.73 kbar and T = 506 °C were calculated on the basis of the thermodynamic dataset compiled by Berman [1991] and Aranovich and Berman [1996]. These values are similar to experimental data: P = 3.76 kbar, T = 501 °C [Holdaway, 1971]. The stability fields of andalusite, sillimanite, and kyanite are used to define pressure boundaries between both metamorphic facies/subfacies and the And-Sil (high thermal T/P gradient) and Ky-Sil (low thermal T/P gradient) metamorphic facies series. Mineral reactions in metapelites which cause the appearance or disappearance of, e. g., garnet+cordierite, orthopyroxene+sillimanite +quartz parageneses play the same role in defining the pressure boundaries. Another fact taken

Table 1. Mineral abbreviations and other symbols

Symbol	Full name	Symbol	Full name	Symbol	Full name
Ab	Albite	Frs	Fersmite	Phl	Phlogopite
Act	Actinolite	Fs	Ferrosillite	Phn	Phengite
Adr	Andradite	Fsp	Feldspar	Pl	Plagioclase
Aeg	Aegirine	Fu	Fuchsite	Po	Pyrrhotite
Alm	Almandine	Gd	Gedrite	Pre	Prehnite
Als	Aluminium silicate	Ghn	Gahnite	Prl	Pyrophyllite
Am	Amphibole	Gl	Glaucophane	Prp	Pyrope
Ame	Amesite	Gn	Galena	Ps	Pistacite
An	Anorthite	Gr	Garnet	Pum	Pumpellyite
And	Andalusite	Grs	Grossular	Px	Pyroxene
Ank	Ankerite	Gru	Grunerite	Py	Pyrite
Ann	Annite	Gt	Graphite	Qu	Quartz
Ant	Anthophyllite	Hb	Hornblende	Rbd	Rhabdophane
Ap	Apatite	Hd	Hedenbergite	Rbk	Riebeckite
Apy	Arsenopyrite	He	Hercynite	Rht	Richterite
Ara	Aragonite	Hl	Halite	Ro	Rhodonite
Arf	Arfvedsonite	Hm	Hematite	Rpd	Ripidolite
Atg	Antigorite	Hq	Holmquistite	Rsm	Rossmanite
Aug	Augite	Hs	Hastingsite	Rt	Rutile
Bd	Baddeleyite	Hy	Hypersthene	Sap	Sapphirine
Bo	Bornite	Im	Ilmenite	Sch	Scheelite
Bre	Breunnerite	Irt	Ilmenorutile	Scp	Scapolite
Brr	Barroisite	Jd	Jadeite	Sid	Siderite
Brt	Barite	Ka	Kaolinite	Sil	Sillimanite
Bt	Biotite	Kfs	K-feldspar	Slc	Silica amorphous
Bz	Bronzite	Kor	Kornerupine	Smt	Smithsonite
Cal	Calcite	Krs	Kersutite	Sp	Spinel
Cc	Chalcocite	Kt	Kataphorite	Sph	Sphalerite
Cch	Clinochlore	Ky	Kyanite	Sps	Spessartine
Cel	Celadonite	L	Liquid phase	Srp	Serpentine
Chl	Chlorite	Le	Lepidolite	St	Staurolite
Chm	Chamosite	Lex	Leucoxene	Stp	Stilpnomelane
Chr	Chromite	Lm	Limonite	Str	Strontianite
Cmb	Columbite	Lw	Lawsonite	Sym	Symplektite
Cob	Cobaltite	Ma	Margarite	Tan	Tantalite
Coe	Coesite	Mag	Magnesite	Tc	Talc
Cor	Corundum	Mb	Molybdenite	Tht	Thorite
Cp	Chalcopyrite	Mi	Microcline	Tmt	Titanomagnetite
Cpx	Clinopyroxene	Mnt	Montmorillonite	To	Topaz
Crb	Carbonate	Mnz	Monazite	Tr	Tremolite
Crd	Cordierite	Mr	Marcasite	Ts	Tschermakite
Crt	Carinthine	Mt	Magnetite	Tt	Titanite
Cst	Cassiterite	Mu	Muscovite	Tu	Tourmaline
Ctd	Chloritoid	Ne	Nepheline	Ur	Uraninite
Cum	Cummingtonite	Oam	Orthoamphibole	Usp	Ulvospinel
Czo	Clinozoisite	Ol	Olivine	Uvr	Uvarovite
Di	Diopside	Om	Omphacite	Ver	Vermiculite
Dol	Dolomite	Opq	Opaque minerals	Vs	Vesuvianite

End of Table 1

Symbol	Full name	Symbol	Full name	Symbol	Full name
Dph	Daphnite	Opx	Orthopyroxene	Wn	Winchite
Ed	Edenite	Or	Orthoclase	Wo	Wollastonite
En	Enstatite	Ort	Orthite	WR	Whole rock
Ep	Epidote	Osm	Osumilite	Wt	Wolframite
Fa	Fayalite	Pa	Paragonite	Xen	Xenotime
fl	Fluid	Pe	Pentlandite	Ze	Zeolite
Flu	Fluorite	Pg	Pargasite	Zo	Zoisite
Fo	Forsterite	Pgt	Pigeonite	Zrn	Zircon

into consideration was garnet appearance or disappearance in paragenesis with plagioclase, cummingtonite, hornblende and clinopyroxene in metabasites. Estimation of pressure by this criterion is less certain but rather convenient because it is easy to identify the presence or absence of garnet in Ca-rich mafic rocks. At a moderate pressure and temperature parageneses with cummingtonite and plagioclase gradually disappear, and parageneses with garnet and hornblende appear as their alternative under relatively high pressures. As the pressure increases, cummingtonite and plagioclase are replaced by garnet with progressively increasing Mg content and by hornblende, which is progressively enriched in Al. The Cum+Pl paragenesis thus becomes unstable in high-pressure complexes. Also, orthopyroxene is an important index mineral in mafic rocks at a high pressure and temperature. With increasing pressure, Opx+Pl becomes unstable, and this paragenesis is replaced by Gr+Cpx+Pl and eventually by Gr+Cpx.

Upon revising our earlier scheme [Bushmin, Glebovitsky, 2008], we decided not to distinguish the epidote-amphibolite facies as an independent one, and this facies is instead included in the low-temperature part of amphibolite facies in our newly introduced variant of the scheme. Our reasoning is that the position of the high-T boundary of the epidote-amphibolite facies is very uncertain and depends on many factors. In particular, epidote and chlorite, typical of the epidote-amphibolite facies, can also remain stable in mafic rocks metamorphosed to the amphibolite facies (chlorite – in Mg-rich rocks, and epidote – in Ca-rich rocks). In this case, the characteristic paragenesis of the epidote-amphibolite facies in metabasites is Hb+Ep+Pl+Chl+Qu±Gr, which can also be stable in the low-T part of the amphibolite facies. Only in the rocks of basaltic composition, the absence of epidote may indicate conditions of the amphibolites facies, when epidote eventually disappears at increasing temperature, and when the mineral paragenesis contains more amphibole and calcic plagioclase. Moreover, epidote contains Fe^{3+} and chlorite may also contain minor Fe^{3+}, and their stability is thus very sensitive to the value of oxygen fugacity (fo_2). At increasing fo_2 the field of epidote stability widens significantly towards higher temperatures. Also, in magnesium-rich metapelites, chlorite may remain stable up to the medium-T amphibolite facies. All these considerations made a ground to omit the epidote-amphibolite facies as an independent facies due to the significant uncertainties of its boundaries. Now we regard it as a low-temperature part of the amphibolite facies.

Analysis of experimental data and thermodynamic calculations shows that, on a generalized «universal P-T grid» for various rock types, the boundaries between mineral facies may be only gradual, due to the wide variation in the composition of mineral solid solutions, bulk rock chemistry, and water activity.

The proposed scheme of mineral facies demonstrates only the principal relationships between metamorphic facies and subfacies, with their boundaries often defined not by a single line but rather by a series of closely spaced lines of univariant reactions, in the result of which characteristic mineral parageneses appear or disappear. In a general case, these reactions relate to systems containing K, Na, Ca, Fe, Mg, Al, and Si. The position of univariant boundary lines in P-T space depends on the composition of solid solutions in the MAS, FAS, FMAS, KFMAS, CFMAS and other systems. If other elements, e. g., Mn, Zn, Ti, and Cr, are contained in a system, the stability fields of minerals that contain these elements expand, and the lines of the univariant reactions are accordingly transformed into divariant or multivariant fields. The boundaries become more diffuse and turn into linear tracts. Such effects of additional elements were considered in publications dedicated to this problem [e. g. Spear, 1993; Mahar et al., 1997; White et al., 2000; Tinkham et al., 2001; Ashley, Law, 2015]. Therefore, boundaries between adjacent facies and some subfacies in the scheme are shown not as thin lines but in the form of broad P-T transition zones (Fig. 1). It should be emphasized that the facies boundaries shown in Fig. 1 do

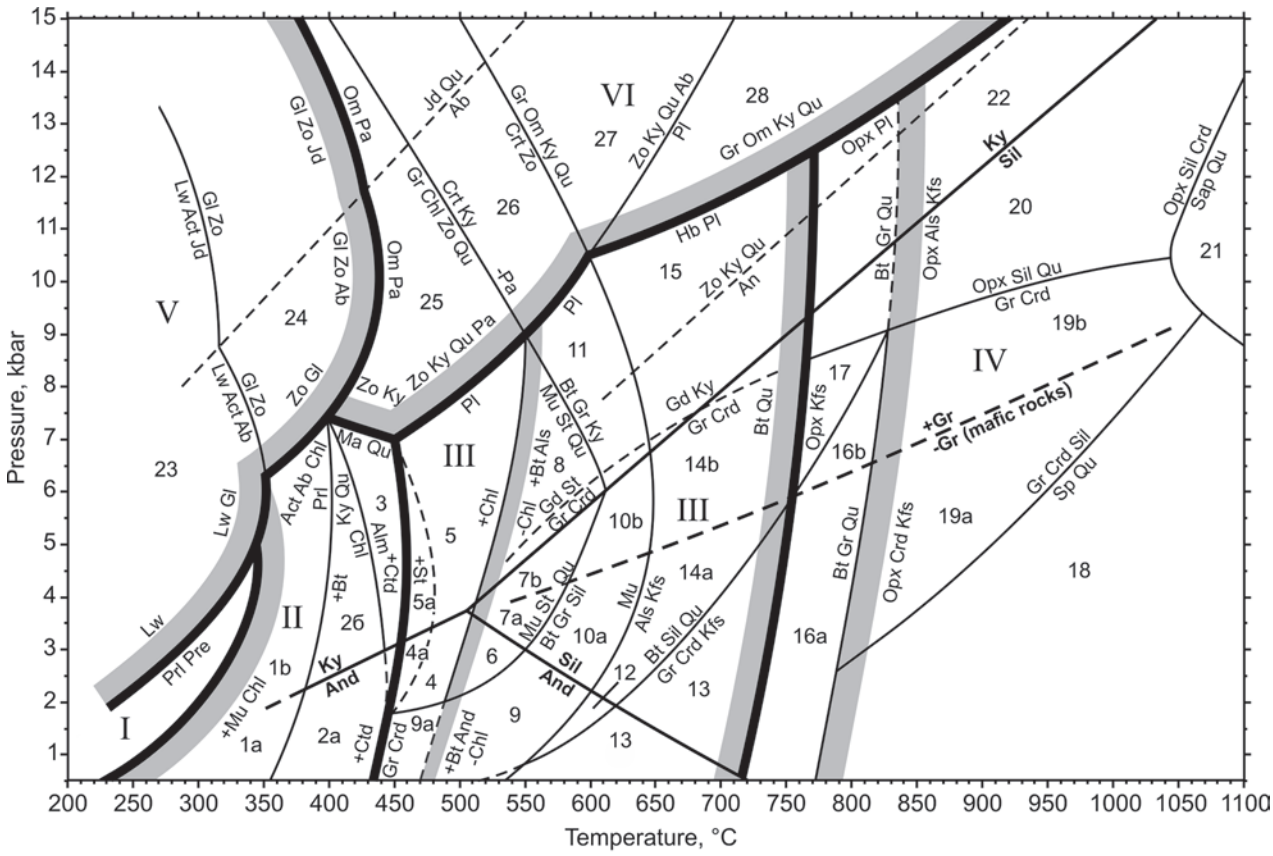

I Prehnite-pumpellyite facies

II Greenschist facies

1. Stilpnomelane-muscovite-chlorite
1a - low-P (And-Sil type)
1b - high-P (Ky-Sil type)

2. Muscovite-chlorite-biotite
2a - low-P (And-Sil type)
2b - high-P (Ky-Sil type)

3. Chlorite-chloritoid-almandine

III Amphibolite facies

4. Andalusite-chlorite-staurolite
4a - low-T zone (Ctd+St stable)
4 - Ctd out, St in

5. Kyanite-chlorite-staurolite
5a - low-T zone (Ctd+St stable)
5 - Ctd out, St in

6. Andalusite-biotite-staurolite
Chl out, Bt+And in

7. Sillimanite-biotite-staurolite
Chl out, Bt+Sil in
7a - low-P (And-Sil type)
7b - high-P (Ky-Sil type)

8. Kyanite-biotite-staurolite
Chl out, Bt+Ky in

9. Andalusite-biotite-muscovite
St out, Bt+And in
9a - low-T zone (Ep, Chl stable)
9 - Ep, Chl out

10. Sillimanite-biotite-muscovite
St out
10a - low-P (And-Sil type)
10b - high-P (Ky-Sil type)

11. Kyanite-biotite-muscovite
St out

12. Biotite-andalusite-orthoclase
Mu out, Kfs+And in

13. Biotite-garnet-cordierite-orthoclase

14. Biotite-sillimanite-orthoclase
Mu out, Kfs+Sil in
14a - low-P (And-Sil type)
14b - high-P (Ky-Sil type)

15. Biotite-kyanite-orthoclase
Mu out, Kfs+Ky in

IV Granulite facies

16. Biotite-garnet-orthoclase-orthopyroxene
Opx+Kfs in
16a - low-P (And-Sil type)
16b - high-P (Ky-Sil type)

17. Biotite-garnet-sillimanite-orthoclase
Opx+Kfs in

18. Quartz-spinel
Opx+Crd+Kfs in, Sp+Qu in

19. Garnet-cordierite-orthoclase-orthopyroxene
Opx+Crd+Kfs in, Gr+Crd in
19a - low-P (And-Sil type)
19b - high-P (Ky-Sil type)

20. Sillimanite-orthopyroxene
Opx+Sil in

21. Quartz-sapphirine
Sap+Qu in

22. Kyanite-orthopyroxene
Opx+Ky in

V Blueschist facies (high to ultrahigh-P)

23. Lawsonite-glaucophane

24. Zoisite-glaucophane

VI Eclogite facies (ultrahigh-P)

25. Paragonite-kyanite-zoisite

26. Zoisite-kyanite-carinthine

27. Garnet-kyanite-omphacite

28. Plagioclase-kyanite-omphacite

— +Gr / -Gr — The line dividing facies and subfacies of Ky-Sil type with a low T/P gradient and of And-Sil type with a high T/P gradient (garnet in/out in mafic rocks)

Fig. 1. Scheme of mineral facies of metamorphic rocks.

Facies – Roman numerals, subfacies – Arabic numerals

not coincide exactly with the experimentally established reaction lines in simplified systems. The boundaries between facies or subfacies which deviate from experimentally validated boundary equilibria at $P_{H2O} = P_{total}$ are consistent with an appreciable decrease in P_{H2O} with depth. We assume [Glebovitsky, 1977; Korikovsky, 1979] that P_{H2O} = 0.5–0.2 P_{total} if the total pressure is higher than 5–6 kbar. These constraints determine the approximate position of curvilinear facies boundaries at variable P_{H2O} under high-temperature and high-pressure conditions. Vast information on the stability of mineral assemblages in real metamorphic complexes with estimated P-T parameters was also taken into account. Our newly obtained and published data [Korikovsky, 1979; Berman, 1991; Powell et al., 1998; Powell, Holland, 2008; Bushmin, Glebovitsky, 2008 and references therein] on particular mineral reactions (experiments, calculations, natural equilibria) make up the basis for the proposed scheme.

2. Scheme of mineral facies of metamorphic rocks

It is difficult to determine the boundary between diagenesis and metamorphism by petrographic criteria. Nevertheless, such a boundary could be established in the rocks according to the first appearance of zones or clusters with newly formed minerals being in physical-chemical equilibrium. Establishing equilibrium requires full recrystallization of the protolith minerals, for example, of clastic and clay fragments, the ordering of the structures of the mica-minerals and an equilibrium distribution of chemical components between the minerals.

Mineral parageneses are defined for various rock types (metapelites, metabasites, etc). We also use the terms «Ca-poor» and «Ca-rich» rocks, which have no genetic sense. The group of «Ca-poor» rocks comprises rock types in which Ca is contained mostly in plagioclase and, sometimes, in minor carbonates, and epidote (Al-metapelites, K-metapelites, K-poor metapelites, Mg-metapelites, K-metasandstones, metasandstones, metagranites, etc). The «Ca-rich» rocks group includes various rocks in which Ca is accommodated in rock-forming minerals (metamafic rocks or metabasites, for example, metabasalts, metaandesites, basic tuffs, basic metasandstones, some metagreywackes, metadiorites, metagabbros, etc). The mineral parageneses of calc-silicate rocks are described separately.

2.1. Prehnite-pumpellyite (or zeolite) facies

In this lowermost temperature facies of relatively low pressure (Fig. 1) the metamorphic recrystallization of whole rock is often feeble and mineral equilibria are often not reached on the whole-rock scale. In fact, this mineral assemblage consists of relic and newly formed metamorphic minerals. Rocks of this facies typically exhibit local alterations with equilibria often reached along fractures in the primary magmatic or sedimentary rocks. The facies is characterized by the presence of prehnite and pumpellyite in various parageneses with chlorite, zeolites (analcime, laumontite, stilbite, and wairakite), actinolite (at higher pressure and temperature), and albite in volcanic rocks and by the presence of kaolinite, hydromuscovite, montmorillonite, and vermiculite in metapelites.

2.2. Greenschist facies

In this low-temperature metamorphic facies (Fig. 1) muscovite, biotite and garnet first appear. Parageneses with chlorite and chloritoid become abundant in Ca-poor rocks. In Ca-rich rocks, assemblages of actinolite with epidote (or zoisite), albite and chlorite are stable. In calc-silicate rocks, the calcite+dolomite+quartz paragenesis is stable. Other minerals such as clinozoisite, chlorite, ankerite and scapolite may also be stable. At the low-temperature boundary of the greenschist facies, hydromicas, montmorillonite, and vermiculite disappear completely in metapelites, and chlorite+muscovite paragenesis appears. Kaolinite decomposes in Al-rich rocks and produces pyrophyllite. In metabasites the breakdown of prehnite and pumpellyite produces parageneses with actinolite, epidote, chlorite, albite, paragonite and carbonate. In this facies, the *stilpnomelane-muscovite-chlorite* (the first chlorite+muscovite), *muscovite-chlorite-biotite* (the first biotite) and *chlorite-chloritoid-almandine* (the first garnet) subfacies can be distinguished.

Stilpnomelane-muscovite-chlorite subfacies (1) (here and below, Arabic numerals of subfacies correspond to those in Fig. 1). In Ca-poor rocks quartz, chlorite, muscovite, albite, stilpnomelane, pyrophyllite, carbonates (ankerite and calcite), kaolinite, talc, paragonite, and occasional microcline are stable, whereas chloritoid, garnet, and biotite are unstable. In Ca-rich rocks quartz, albite, carbonates, chlorite, epidote, zoisite, actinolite are stable.

Muscovite-chlorite-biotite subfacies (2). Biotite is stable and widespread in K-metasandstones. Stilpnomelane gradually disappears in metapelites, and the first paragenesis with low-Al biotite appears: Stp+Chl+Mu = Bt+Mu. The first high-Fe chloritoid as a product of the reaction Chl_{Fe}+Prl = Ctd_{Fe}+Qu can appear at approximately the same temperature in high-Al metapelites.

The first aluminum silicates (andalusite, kyanite) appear in high-Al metapelites as products of pyrophyllite dehydration. In Ca-poor rocks biotite, muscovite, phengite, chlorite, chloritoid, stilpnomelane, microcline, carbonates (ankerite and calcite), talc, albite and cummingtonite (in K-poor rocks) are stable. The assemblage of biotite with chloritoid is however unstable. In Ca-rich rocks quartz, albite, carbonates, epidote, clinozoisite, and chlorite are stable. Pale-colored hornblende may appear together with colorless actinolite, and pumpellyite disappears completely.

Chlorite-chloritoid-almandine subfacies (3) is typical of kyanite-type greenschist complexes. In andalusite-type complexes, this subfacies occurs only in a small high-temperature part of the greenschist facies. Under the conditions of this subfacies, the first Fe-rich garnet (almandine) appears as a product of Fe-chlorite breakdown in the reaction $Qu+Chl_{Fe} = Gr_{Fe}$. With increasing temperature, the Mg-content of garnet and chlorite increases. As pressure increases, the reaction of chlorite decomposition shifts toward low temperatures (Fig. 1). Thus, at a higher pressure (more than ~5 kbar), the first garnet (almandine) gradually appears together with the first biotite. The paragenesis of almandine, chlorite and chloritoid is critical for this subfacies. Thus, chloritoid, kyanite (andalusite), chlorite, muscovite, almandine, albite, biotite, stilpnomelane, and cummingtonite (in K-poor rocks) are stable in Ca-poor rocks. At the same time, assemblages biotite+andalusite (or kyanite) and biotite+chloritoid are unstable. In Ca-rich rocks colorless actinolite sometimes with pale-colored hornblende is stable, as well as chlorite, epidote, carbonates, albite, and garnet.

2.3. Amphibolite facies

The low-T boundary of amphibolite facies (Fig. 1) in metapelites at a pressure higher than 2 kbar is defined by the appearance of staurolite due to the gradual breakdown of chloritoid (transition to *subfacies 4* and *5*). Iron-richest chloritoid is the first to disappear. In the KFMAS system, the boundary is not a single line but a series of closely spaced lines of mineral reactions within a narrow T interval. As temperature increases in the field of andalusite stability, the reactions are: Ctd+Chl+And = St+Qu, Ctd+And+Qu = St+Gr, Ctd+Chl+Qu = St+Gr, and Ctd+Qu = St+Chl+Gr. In the field of kyanite stability the reactions are: Ctd+Chl+Ky = St+Qu, Ctd+Chl+Mu = St+Bt+Qu, Ctd+Ky+Qu = St+Gr, Ctd+Mu+Qu = St+Bt+Gr, and Ctd+Qu = St+Gr+Ky. In a very narrow temperature interval (within the Ky field) the biotite+chloritoid paragenesis can be stable: Gr+Chl+Mu = Bt+Ctd+Qu. In Mg-metapelites, mainly in the field of andalusite stability, the first cordierite may appear as a product of the reaction Phl+Als = Crd_{Mg}+Mu. At pressures lower than 2 kbar, where staurolite is completely unstable, the low-T boundary with the greenschist facies is defined by a series of closely spaced reaction lines in the narrow temperature *transition zone 9a*: Ctd+Qu = Gr+Crd+Chl, Ctd+Qu=Chl+Gr+And, And+Chl+Qu = Gr+Crd, and Chl+Mu+Qu = Bt+Crd. As a consequence, chloritoid disappears, chlorite disappears gradually, and parageneses of cordierite with garnet and biotite with andalusite appear in *subfacies 9*: Chl+Mu+Qu = Gr+Crd+Bt and Gr+Chl+Mu = Bt+And+Qu.

In metabasites, actinolite disappears, and the parageneses of bluish green hornblende with epidote, plagioclase (oligoclase), chlorite and garnet are stable. Garnet is however less typical, and even completely absent at a low pressure if the rocks are not rich in Fe. Increasing pressure widens the field of epidote (clinozoisite, zoisite)+plagioclase stability towards high temperatures (*subfacies 5*).

The wide temperature range of this facies (from ~450 to ~750 °C) enables the subdivision of the amphibolite facies into low-, medium- and high-T parts. The abundance of various metapelitic assemblages sensitive to variation in P-T conditions makes it possible to distinguish a series of temperature subfacies at different pressures.

<u>The low-T part of the amphibolite facies</u> (*subfacies 5, 4*) is the stability field of staurolite-bearing mineral assemblages together with chlorite in metapelites. The parageneses chlorite+staurolite±garnet and chlorite+cordierite are widespread. At a very low pressure (*zone 9a of subfacies 9*), the paragenesis garnet+cordierite without staurolite appears for the first time among chlorite assemblages. Parageneses of bluish green and green hornblende with epidote, chlorite, plagioclase (albite-oligoclase), and garnet (Fe-rich rocks) are stable in metabasites. These rocks are characterized by an abundance of equilibrium chlorite. In calc-silicate rocks the dolomite+quartz paragenesis may be preserved or alternative tremolite+calcite paragenesis appears. Other minerals such as hornblende, chlorite, clinozoisite, zoisite, ankerite, scapolite, and garnet (grossular-andradite) may also be stable.

Subfacies 4 and *5* correspond to different pressure conditions. The *andalusite-chlorite-staurolite subfacies (4)* is characterized by the stability of muscovite, biotite, andalusite, staurolite, cordierite, garnet, anthophyllite (in K-poor rocks), and chlorite. The *kyanite-chlorite-staurolite subfacies (5)* is characterized by the stability of muscovite, staurolite, biotite, kyanite, garnet, chlorite, and

cordierite (only at moderate P near the andalusite field). Cummingtonite is stable in K-poor rocks in both subfacies. There is a narrow temperature zone (~450–480 °C) in *subfacies 4* and *5* in which the parageneses chloritoid+staurolite and chloritoid+biotite are stable in high-Al metapelites up to the complete decomposition of chloritoid (*transition zones 4a* and *5a*). The assemblage cordierite+staurolite is unstable within the entire temperature interval of *subfacies 4* and *5.*

The medium-T part of the amphibolite facies (Fig. 1) in metapelites encompasses the stability field of staurolite-bearing assemblages (*subfacies 6, 7, 8*), after chlorite disappearence in the rocks with a medium Mg content, and the stability field of two-mica with alumina silicates assemblages (*subfacies 9, 10, 11*) after complete disappearance of staurolite and the «last» chlorite (in Mg-rich rocks). In *subfacies 6, 7, 8* the assemblage of staurolite with cordierite and without chlorite develops for the first time, but it is abundant only in low-P metapelites of andalusite-sillimanite complexes (*subfacies 6, 7a*). For the first time, the parageneses of biotite+aluminum silicates (kyanite or andalusite or sillimanite) appear at moderate to high pressures in staurolite-bearing rocks and at low pressures (less than 2 kbar) in staurolite-free biotite-garnet schists. In Ca-rich rocks epidote and chlorite disappear from the hornblende assemblages, except for the situations discussed above. In calc-silicate rocks clinopyroxene (diopside) first appears after the breakdown of dolomite+quartz and tremolite+calcite+quartz assemblages. As a result, diopside or alternative tremolite+calcite+quartz paragenesis may be stable. At higher temperature in quartz-free rocks clinopyroxene together with calcite and tremolite are stable. Other minerals such as hornblende, clinozoisite, zoisite, scapolite, and garnet (grossular-andradite) may also be stable. Also, it is noteworthy that at low pressures (*subfacies 9, 6*) the medium-T part of the amphibolite facies begins at a temperature around 480–500 °C, whereas at high pressures (*subfacies 8*) it begins at ~550 °C.

The transition to the medium-T part of the amphibolite facies (to *subfacies 6, 7, 8* and *9, 10, 11*) in metapelites is defined by the disappearance of chlorite-bearing assemblages in the staurolite stability field and by the first appearance of biotite in parageneses with aluminum silicates (andalusite, sillimanite, and kyanite). This transition is via a series of closely spaced lines of mineral reactions. In the field of kyanite stability these reactions are: St+Chl+Mu = Bt+Ky+Qu, Gr+Chl+Mu = Bt+Ky+Qu, St+Chl+Qu = Gr+Crd (narrow P-T space), Ky+Chl+Qu = St+Crd, Chl+Mu+Qu = Bt+Crd, Chl+Mu+Qu = Bt+Crd+Ky (at moderate pressure), and Chl+Mu = Bt+Ky+Qu. In the field of andalusite stability these reactions are: St+Chl+Mu = Bt+And+Qu, St+Chl+Qu = Gr+Crd, And+Chl+Qu = St+Crd, Chl+Mu+Qu = Bt+Crd, and Chl+Mu+Qu = Bt+Crd+And. Outside the staurolite stability field at pressures less than 2 kbar, after chlorite disappearance in the transition zone 9a, the paragenesis of biotite and andalusite appears also in *subfacies 9*: Gr+Chl+Mu = Bt+And+Qu. But in Mg-metapelites, Mg-chlorite with muscovite, biotite and andalusite can still be stable.

Depending on pressure, the staurolite stability field without chlorite can be subdivided into the *andalusite-biotite-staurolite (6), sillimanite-biotite-staurolite (7),* and *kyanite-biotite-staurolite (8) subfacies*. These staurolite-bearing subfacies in metapelites are characterized by the stability of staurolite, muscovite, biotite, kyanite (sillimanite, andalusite), garnet, cummingtonite (K-poor rocks), gedrite (K-poor rocks in kyanite field), anthophyllite (K-poor rocks in andalusite field), and cordierite. At the same time, the assemblage biotite+garnet+kyanite (sillimanite, andalusite) is unstable in all these subfacies. Cordierite is abundant mainly in the field of andalusite and sillimanite stability *(subfacies 6 and 7)*. Cordierite together with garnet is unstable in kyanite field *(subfacies 8)*. However, this assemblage is stable under a lower pressure together with sillimanite *(subfacies 7)* or andalusite *(subfacies 6)*. Bluish green hornblende, plagioclase, garnet, clinopyroxene, cummingtonite, and in certain situations also epidote, zoisite, chlorite *(subfacies 6),* and carbonates are stable in Ca-rich rocks.

Depending on pressure, two-mica with alumina silicates parageneses can be subdivided into the *andalusite-biotite-muscovite (9)*, *sillimanite-biotite-muscovite (10),* and *kyanite-biotite-muscovite (11) subfacies*. The boundary between *subfacies 6, 7, 8* and *subfacies 9, 10, 11* is identified by the disappearance of staurolite and Mg-chlorite: St+Mu+Qu = Bt+Gr+Ky (Sil, And), St+Qu = Gr+Gd+Ky, St+Qu = Gr+Crd+Sil, St+Qu = Gr+Crd+And, and Chl_{Mg}+Mu = Phl+Als. Around this boundary, the univariant Bt+Als+Gr+St+Mu+Qu paragenesis can exist and is commonly found in metapelites. In K-metapelites (muscovite-bearing schists) staurolite disappears at a temperature (maximum ~600–620 °C) lower than that in K-poor metapelites (maximum ~650 °C), in which, for example, an alternative paragenesis of gedrite, kyanite and garnet is formed at a high pressure. *Subfacies 9, 10, 11* in Ca-poor rocks are characterized by the stability of andalusite (sillimanite, kyanite), biotite, muscovite, garnet, cordierite, cummingtonite (K-poor rocks), plagioclase, and gedrite (K-poor rocks in the field of

andalusite and sillimanite). Cordierite is stable and abundant mainly in the field of andalusite and sillimanite (*subfacies 9 and 10*), whereas in the field of kyanite *(subfacies 11)* this mineral can be stable in Al-, Mg-metapelites. Cordierite together with garnet are not stable in the field of kyanite *(subfacies 11)*, and at a lower pressure, they are stable with sillimanite *(subfacies 10)* and andalusite *(subfacies 9)*. In the low-temperature part of the low-pressure *andalusite-biotite-muscovite subfacies (9),* chlorite can be preserved in Mg-metapelites. In K-poor rock*s* containing gedrite and cummingtonite, Fe-orthopyroxene appears for the first time as a product of the reactions Cum+Gr = Gd+Opx, Gr+Gd = Opx+Qu, and Cum+Mt = Opx+Qu.

The medium-T subfacies of the amphibolite facies in metabasites are defined by the disappearance of epidote and chlorite from hornblende-plagioclase (oligoclase-andesine) assemblages and appearance of the Hb±Cpx+Gr+Pl paragenesis of the high-P amphibolite facies in the kyanite-syllimanite type of metamorphism *(subfacies 7b, 10b, 14b, 8, 11, 15)*, and the Hb±Cpx+Cum+Pl paragenesis of low-P amphibolite facies in the andalusite-sillimanite type of metamorphism *(subfacies 7a, 10a, 14a, 6, 9, 12)*. As pressure decreases, garnet and aluminous hornblende disappear gradually from the assemblages of these subfacies. At first, parageneses with low-Al hornblende, cummingtonite, garnet and plagioclase appear. Then low-P parageneses without garnet begin to form. Occasionally, in the medium-T part of the amphibolite facies, Mg-chlorite remains in parageneses with hornblende. The disappearance or existence of epidote containing Fe^{3+} depends on fo_2.

The high-temperature part of the amphibolite facies, in which anataxis and migmatization of rocks start to develop, is the P-T stability field of orthoclase-bearing assemblages with biotite and aluminum silicates as products of muscovite breakdown before the appearance of orthopyroxene in metapelites *(subfacies 12, 13, 14, 15)*. Zones with rocks bearing the sillimanite+orthoclase paragenesis are sometimes called second sillimanite zones. In metabasites, hornblende parageneses with plagioclase and clinopyroxene are widespread. Depending on pressure and Fe content, cummingtonite and garnet appear in or disappear from these parageneses. In calc-silicate rocks the assemblage Cal+Tr disappears and parageneses with clinopyroxene become abundant. Hornblende, plagioclase and calcite are stable. At higher temperature forsterite becomes stable. Other minerals such as scapolite, garnet (grossular-andradite), and dolomite may also be stable.

Depending on pressure, this part of the amphibolite facies is subdivided into the *biotite-andalusite-orthoclase (12)*, *biotite-garnet-cordierite-orthoclase (13)*, *biotite-sillimanite-orthoclase (14),* and *biotite-kyanite-orthoclase (15) subfacies*. The boundary between *«muscovite» (9, 10, 11) and «orthoclase» (12, 13, 14, 15) subfacies* is identified by the complete disappearance of muscovite. In Ca-rich rocks epidote, zoisite, and chlorite disappear completely; and brown-green hornblende, plagioclase, garnet, clinopyroxene and cummingtonite are stable. In K-poor rocks, cummingtonite, anthophylite (commonly in the field of andalusite) and gedrite (in the field of sillimanite and kyanite) as well as Fe-orthopyroxene can occur. The *biotite-andalusite-orthoclase subfacies (12)* occupies a small field, in which the biotite+andalusite+orthoclase paragenesis may contain cordierite and garnet. However, garnet, cordierite and orthoclase are unstable if occurring together. The *biotite-sillimanite-orthoclase subfacies (14)* occupies an extensive field, in which the biotite-sillimanite-orthoclase paragenesis may also contain cordierite and garnet, but the Gr+Crd+Kfs assemblage is unstable here similar to *subfacies 12*. The boundary of the *biotite-garnet-cordierite-orthoclase subfacies (13)* with *subfacies 12* and *14* is determined by the disappearance of the Bt+Sil (And)+Qu paragenesis. Under the conditions of *subfacies 13*, biotite, garnet, cordierite, sillimanite (andalusite) and orthoclase are stable in various combinations, except only for Bt+Als+Qu. Around this boundary the univariant Bt+Sil+Gr+Crd+Kfs paragenesis can exist. Biotite, kyanite, garnet and orthoclase are stable under the conditions of the *biotite-kyanite-orthoclase subfacies 15*. In this subfacies cordierite is of limited abundance in Mg-rich metapelites and the garnet+cordierite assemblage is unstable.

2.4. Granulite facies

In general, this is a P-T stability field for the orthopyroxene-orthoclase paragenesis in Ca-poor rocks and orthopyroxene-clinopyroxene-plagioclase paragenesis with garnet (at higher pressure) or without garnet (at lower pressure) in Ca-rich rocks (Fig. 1). The low-T boundary of granulite facies in Ca-poor rocks is defined by the gradual appearance of the orthopyroxene+orthoclase paragenesis as a breakdown product of low-Al and low-Mg biotite by the reaction Bt+Qu = Kfs+Opx and/or by dehydration melting. The further transition at increasing temperature to orthoclase-cordierite-orthopyroxene granulite is related to the gradual decomposition of high-Al and relatively low-Mg biotite: Bt+Gr+Qu = Kfs+Crd+Opx.

In Mg-rich rocks, however, biotite is preserved. Ca-free amphibole disappears completely. Under the same T-conditions, hornblende and cummingtonite disappear from mineral assemblages in Ca-rich rocks. At higher pressure, the Cpx±Opx+Gr+Pl paragenesis of high-P granulite facies *(subfacies 16b, 17, 19b, 20, 21, 22)* appears due to intensive growth of garnet at increasing pressure. But at lower pressure, the garnet-free Cpx±Opx+Pl paragenesis of moderate- and low-P granulite facies *(subfacies 16a, 19a, 18)* is stable. Hornblende breakdown depends on water activity, quartz content in the rock and on its Mg content. That is why hornblende often occurs in granulites. In calc-silicate rocks clinopyroxene, calcite, forsterite, plagioclase, hornblende, garnet (grossular-andradite), and wollastonite may be stable. Wollastonite can appear in these rocks as a result of the reaction Cal+Qu = Wo.

The granulite facies is subdivided into the *biotite-garnet-orthoclase-orthopyroxene (16), biotite-garnet-sillimanite-orthoclase (17), quartz-spinel (18), garnet-cordierite-orthoclase-orthopyroxene (19), sillimanite-orthopyroxene (20), quartz-sapphirine (21), and kyanite-orthopyroxene (22) subfacies*.

The *biotite-garnet-orthoclase-orthopyroxene (16)* and *biotite-garnet-sillimanite-orthoclase (17) subfacies* are the transitional low-T part of the granulite facies at low and moderate pressures, where the breakdown of biotite in Ca-poor rocks initiates the formation of the stable assemblage of orthopyroxene and orthoclase, but still without cordierite, which will appear in this paragenesis at a higher temperature. Orthopyroxene, high-Al and high-Ti biotite, sillimanite, garnet, cordierite, and orthoclase are stable under the conditions of these subfacies. However, Opx+Sil, Opx+Crd+Kfs, and Gr+Crd+Kfs assemblages are unstable in *subfacies 17*, and the Opx+Sil and Opx+Crd+Kfs assemblages are unstable in *subfacies 16*. Around the boundary between *subfacies 16* and *17* the univariant Bt+Sil+Gr+Crd+Kfs paragenesis is possible for several reasons, including the expansion of the garnet stability field due to variation in the Ca and Mn contents and the expansion of the biotite stability field due to variation in Fe, Al and Ti. In Ca-rich rocks, garnet in paragenesis with pyroxenes and brown hornblende is common only in *subfacies 17* and *16b*, whereas in *subfacies 16a* garnet disappears completely at pressures decreasing from moderate to low.

The *quartz–spinel (18)* and *garnet-cordierite-orthoclase-orthopyroxene (19) subfacies* occupy the high-temperature part of the granulite facies at low and moderate pressures. These high-T granulites are characterized by the disappearance of sillimanite and garnet assemblages with low-Mg high-Al biotite and the appearance of the orthopyroxene+orthoclase+cordierite paragenesis. Orthopyroxene, garnet, cordierite, sillimanite, orthoclase, and spinel (with quartz only in *subfacies 18*) are stable under the conditions of *subfacies 18* and *19*, but the Opx+Sil+Qu assemblage is unstable, and the Gr+Crd+Sil assemblage is stable only in *subfacies 19*. It should be noted that Zn-bearing spinel, which is not rare in granulites, can also be stable with quartz at much higher pressures and lower temperatures than in *subfacies 18.* Mg-rich biotite may occur in K-metapelites together with orthoclase and orthopyroxene up to ~850–900 °C and then it disappears gradually by the reactions Bt_{FeMg}+Qu = Bt_{Mg}+Opx+Crd+Kfs and Bt_{Mg}+Qu = Opx_{Mg}+Crd_{Mg}+Kfs. In Ca-rich rocks, garnet in association with pyroxenes and brown hornblende is typical only of the high-P part (*subfacies 19b*) of the *garnet-cordierite-orthoclase-orthopyroxene subfacies (19).* When pressure drops, garnet disappears from the parageneses with pyroxenes and hornblende *(subfacies 19a)* and is as a rule absent in Ca-rich parageneses of the quartz-spinel *subfacies (18)*.

The *sillimanite-orthopyroxene (20), quartz-sapphirine (21) and kyanite-orthopyroxene (22) subfacies* occupy the high-T and high-P (more than ~9 kbar) part of the granulite facies. The low-P boundary of the *sillimanite-orthopyroxene subfacies (20)* is defined by the disappearance of the Gr+Crd assemblage and the appearance of the alternative Opx+Sil+Qu paragenesis. The high-P boundary of the *sillimanite-orthopyroxene subfacies (20)* with *kyanite-orthopyroxene subfaces (22)* is defined by the appearance of the Ky+Opx paragenesis at the phase transition of sillimanite into kyanite and, as a result, the breakdown of the most magnesian «last» cordierite: Crd_{Mg} = Opx_{Mg}+Ky+Qu.

In the low-T part of the *sillimanite-orthopyroxene (20) and kyanite-orthopyroxene (22) subfacies* near the boundary with the amphibolite facies, the stable mineral assemblage consists of orthopyroxene, sillimanite (kyanite), quartz and garnet, but without orthoclase. Orthoclase appears in this paragenesis at increasing temperature as a product of the reaction Bt+Gr+Qu = Opx+Als+Kfs. Under the conditions of *subfacies 20* and *22*, biotite, orthopyroxene, garnet, sillimanite (kyanite), cordierite (only *in subfacies 20*), sapphirine, orthoclase, and spinel are stable in Ca-poor rocks, but the assemblages sapphirine+quartz, spinel+quartz, and cordierite+garnet are unstable. As in the low-pressure granulite subfacies, the preservation of biotite depends on the contents of Mg, Al, Ti, and water

activity, so that the Bt+Opx+Sil+Kfs+Qu paragenesis is preserved in, for example, Mg-metapelites. In Ca-rich rocks, the stable mineral assemblage consists of pyroxenes, brown hornblende (only in the low-T region), garnet, and plagioclase.

The Qu+Sap paragenesis is the main criterion for recognition of the *quartz-sapphirine subfacies (21)*. Its boundary with the *sillimanite-orthopyroxene subfacies (20)* is determined by the reaction Opx+Sil+Crd = Sap+Qu; the boundary with the *garnet-cordierite-orthoclase-orthopyroxene subfacies (19)* by the reaction Crd+Gr+Sil = Sap+Qu; and the boundary with the *quartz-spinel subfacies (18)* by the reaction Sp+Crd+Sil = Sap+Qu. Under the conditions of the *quartz-sapphirine subfacies (21)*, the following minerals are stable in various combinations: sapphirine, biotite, orthopyroxene and sillimanite (sillimanite together with orthopyroxene only in the restricted high-pressure part of this subfacies), garnet and cordierite (only in the low-temperature part near the boundary with *subfacies 19*), orthoclase and spinel (spinel together with quartz only in the restricted part of relatively low pressure).

2.5. Blueschist (or glaucophane-schist) facies

The blueschist facies (Fig. 1) is a temperature analogue of the prehnite-pumpellyite and greenschist facies at high- and ultrahigh-P. The parageneses of glaucophane, lawsonite, muscovite, phengite and pumpellyite with such typical greenschist minerals as actinolite, zoisite, pyrophylite, chlorite, garnet, paragonite, stilpnomelane, albite, epidote, calcite, and quartz are stable in Ca-rich rocks. At pressures higher than ~8–11 kbar, almost pure jadeite may appear in paragenesis with quartz. The *lawsonite-glaucophane subfacies (23)* corresponds to the lowest temperature conditions such as in prehnite-pumlellyite and the low greenschist facies, but at high-P (up to 12–13 kbar). The *zoisite-glaucophane subfacies (24)* at temperatures of the prehnite-pumlellyite and greenschist facies corresponds to even higher pressures, up to 13–15 kbar.

The boundary of the *lawsonite–glaucophane subfacies (23)* with the prehnite-pumpellyite facies and partly with the greenschist facies is determined by the reactions Pr+Prl = Lw+Qu, Pr+Cal = Lw+Zo and Chl+Ab = Gl, Act+Chl+Ab+Qu = Lw+Gl. As a result, the parageneses of lawsonite and glaucophane with chlorite and albite, with calcite and albite, or with calcite and chlorite, which are typical of this subfacies, appear.

The boundary of the *zoisite–glaucophane subfacies (24)* with the greenschist facies is determined by the reactions Act+Chl+Ab = Gl+Zo+Qu and Act+Chl+Pa+Ab = Zo+Gl. Consequently, parageneses of zoisite or epidote and glaucophane with actinolite and albite, with chlorite and albite, and with chlorite and actinolite become common.

The boundary between *subfacies 23* and *24* is established by the appearance of zoisite (epidote)+glaucophane paragenesis and gradual disappearance of lawsonite: Lw+Act+Ab = Zo+Gl and Lw+Act+Jd = Zo+Gl (these reactions are assumed as a boundary), Lw+Qu = Zo+Prl. At increasing temperature, the paragenesis of glaucophane and paragonite appears by the reaction Chl_{Al}+Ab = Gl+Pa. Also, transitional parageneses of zoisite and glaucophane with chlorite and pargasite, pargasite and omphacite, or omphacite and albite can appear near the high-temperature boundary with the eclogite facies (*subfacies 25*). It is worth noting however that the boundary of lawsonite disappearance at increasing T and P depends considerably on H_2O activity. In a scenario with a high value of this parameter ($P_{H2O} \sim P_{total}$), lawsonite remains stable together with glaucophane till the high-T boundary with plagioclase-free zoisite-kyanite-quartz eclogites (*subfacies 25*), in which it breaks down via the reaction Lw = Zo+Ky+Qu. In this case the fields of the *lawsonite–glaucophane subfacies (23) and zoisite–glaucophane subfacies (24)* overlap and the paragenesis of zoisite, kyanite and quartz may appear in the field of glaucophane stability. The appearance of omphacite in blueschists in the transitional zone to plagioclase-free eclogites *(subfacies 25)* is explained in the same way.

2.6. Eclogite facies

The eclogite facies (Fig. 1) is a temperature analogue of the amphibolite and granulite facies at ultrahigh pressures. The widespread paragenesis of omphacite with garnet (typically pyrope and grossular-rich) is characteristic of this facies. The paragenesis of almost pure jadeite with quartz is formed at pressures higher than ~12 kbar. Other minerals such as amphibole (pargasite), epidote, zoisite, kyanite, paragonite, albite, and Na-Ca-plagioclase may also be stable in the eclogite facies. Often rutile occurs there. Parageneses and various mineral reactions in eclogites after different protolith in the transition zone from amphibolite and granulite facies are well documented in many publications [e. g. Korikovsky et al., 1997, 1998a, b, 2004; Korikovsky, 2005, 2009, 2012; Kozlovskii et al., 2015].

Eclogite rocks of the *paragonite–kyanite–zoisite (25), zoisite–kyanite–carinthine (26)* and *garnet–kyanite–omphacite (27) subfacies* with the zoizite+kyanite+quartz paragenesis are sometimes called plagioclase-free eclogites and the rocks of

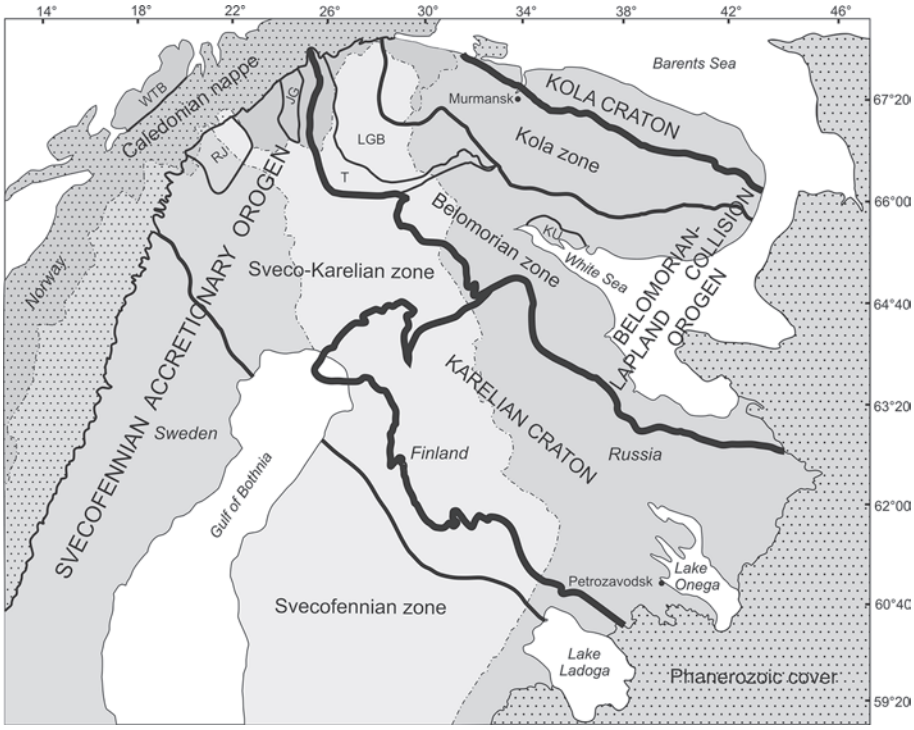

Fig. 2. Major tectonic units of the Fennoscandian Shield.

LGB – Lapland Granulite belt, T – Tana belt

Archean enclaves of the Karelian craton (Archean crust) occurring as relicts within the Sveco-Karelian tectonic zone of the Svecofennian orogen: WTB – West Troms Basement Complex, RJ – Råstojaure complex, JG – Jergul complex

the *plagioclase-kyanite-omphacite subfacies (28)* are called plagioclase eclogites.

The low-temperature boundary of the eclogite facies with the blueschist facies is rather uncertain, because the eclogite mineral assemblage can occur in the high-temperature part of the blueschist facies with glaucophane-bearing assemblages. Glaucophane gradually disappears as a result of mineral transformations, e. g. by the reactions Zo+Gl+Ab = Om+Pa, Zo+Gl+Jd = Om+Pa, Gl+Zo = Pg+Pa, and Gl+Pg+Qu = Om+Gr.

The *paragonite–kyanite–zoisite (25) and zoisite–kyanite–carinthine (26)* eclogite subfacies correspond to the temperature conditions of the low- to medium-T amphibolite facies. In *subfacies 25* parageneses with paragonite, zoisite, kyanite, quartz, omphacite, pargasite, chlorite, and garnet are widespread, but the assemblages pargasite+kyanite, omphacite+kyanite, and omphacite+kyanite+garnet are unstable. The low-pressure boundary with the low amphibolite facies is determined in Ca-rich rocks by the appearance of zoisite in paragenesis with kyanite, quartz, and paragonite as products of margarite and plagioclase decomposition: Ma+Qu = Zo+Ky and Pl_{CaNa} = Zo+Ky+Qu+Pa.

In the *zoisite–kyanite–carinthine subfacies (26)* at increasing temperature paragonite becomes unstable as a result of the reaction Pa+Qu = Ab+Ky, and the carinthine+kyanite paragenesis becomes stable as a result of the reaction Gr+Chl+Zo+Qu = Crt+Ky. Parageneses with carinthine (brown pargasite with high Mg, Ca, Al, Ti contents, typical of eclogites), kyanite, zoisite, omphacite, quartz, albite, and garnet are typical of this subfacies. The low-P boundary, as in *subfacies 25*, is determined by the reaction of plagioclase breakdown: Pl_{CaNa} = Zo+Ky+Qu+Ab. The boundary between the *zoizite–kyanite–carinthine subfacies (26)* and *subfacies 25* is determined by the decomposition of chlorite–zoisite schists with the formation of the parageneses with carinthine and kyanite: Gr+Chl+Zo+Qu = Crt+Ky. Talc in paragenesis with kyanite and muscovite±paragonite (so-called whiteschists) can appear in *subfacies 25 and 26* at the boundary with the amphibolite facies in Mg-metapelites as a product of the reactions Chl_{Mg}+Phl = Tc+Mu, Chl_{Mg} = Tc+Ky, and Ab+Ky = Pa+Qu.

The *garnet–kyanite–omphacite eclogite subfacies (27)* corresponds to the temperature conditions of medium-T amphibolite facies. S*ubfacies 27* includes parageneses of omphacite and garnet with kyanite, zoisite, and quartz, which are products of the breakdown of carinthine in assemblage with zoisite at the boundary with the *zoisite-kyanite-carinthine subfacies (26)* via the reaction Crt+Zo = Om+Gr+Ky+Qu.

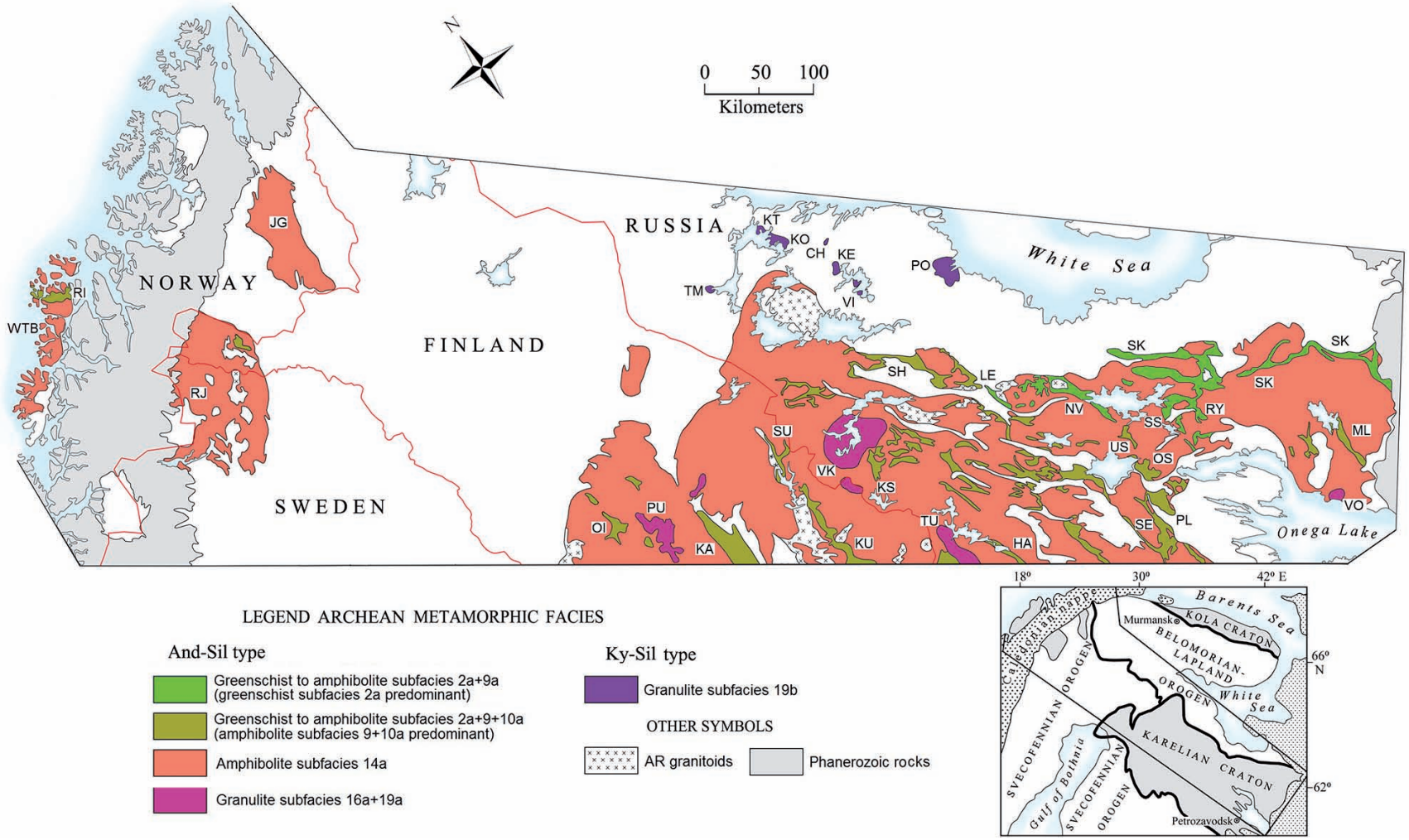

Fig. 3. Simplified map of Archean metamorphism.

Compiled by Sergey Bushmin (RAS), Julio Gonzalez (SGU), Jan Sverre Sandstad (NGU), Elena Savva (RAS).
Uncolored areas correspond to Proterozoic metamorphic and intrusive rocks.
Archean enclaves of the Karelian craton occurring as relicts within the Svecofennian orogen: WTB – West Troms Basement Complex, RJ – Råstojaure complex, JG – Jergul complex.
Granulite areas: PU – Pudosjärvi, VK – Verhnee Kuyto, TU – Tulos, VO – Vodlozero, TM –Tumcha, KT – Kovdozero (Tupaya Guba), KO – Kovdozero, CH – Chupa, KE – Keret', VI – Vichany, PO – Pon'goma
Greenstone belts: RI – Ringvassøya, OI – Oijärvi, KA – Kainuu, KU – Kuhmo, SU – Suomussalmi, HA – Hattu (Ilomantsi), KS – Kostomuksha, SH – Shombozero, LE – Lehta, US – Urosozero, OS – Oster, PL – Palalambi, SE – Semcha, ML – Matkalahti, NV – North Vygozero, SS – Shilos, RY – Rybozero, SK – Sumozero–Kenozero.
The inset shows the location of the study area

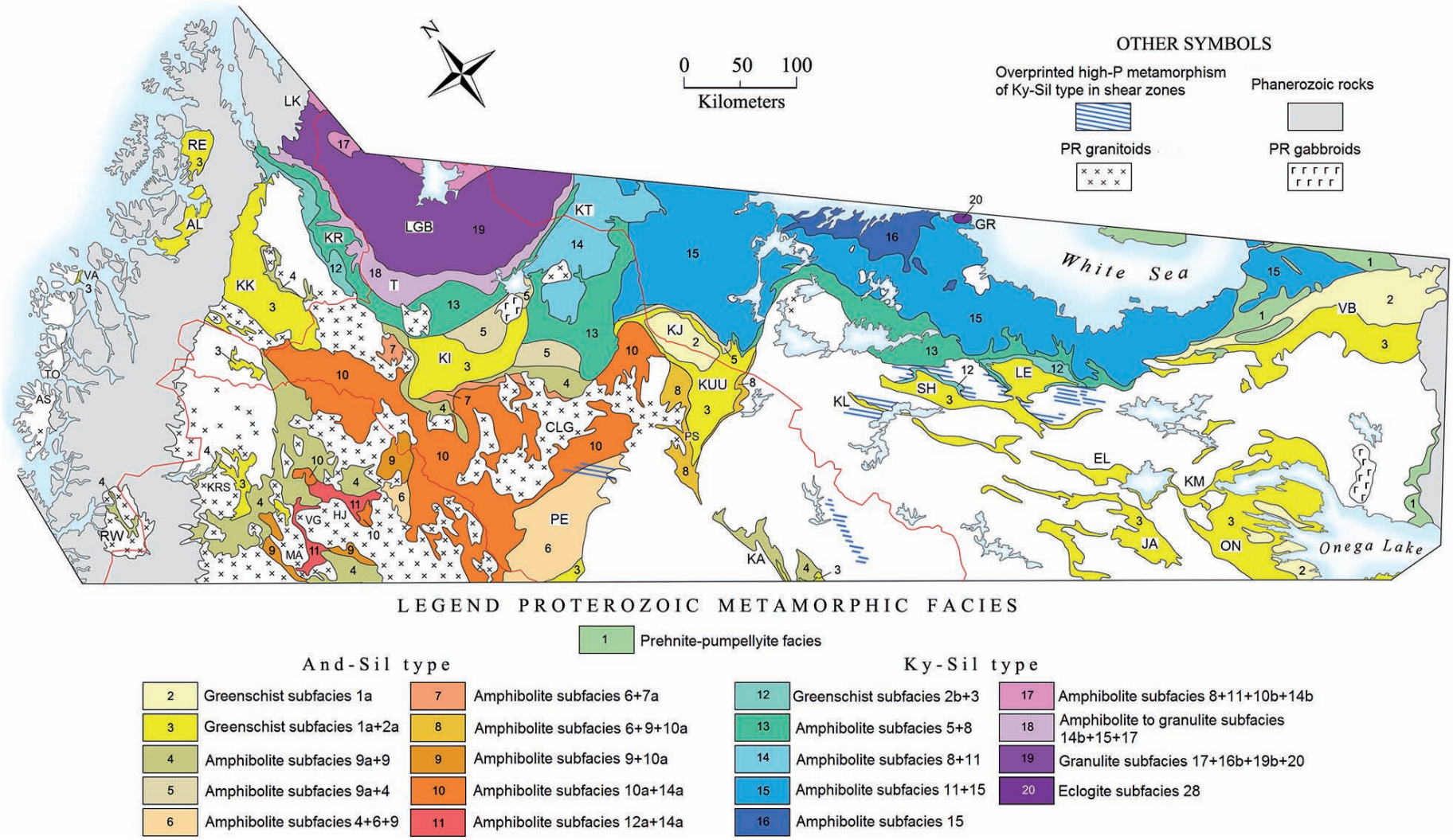

Fig. 4. Simplified map of Proterozoic metamorphism.

Compiled by Sergey Bushmin (RAS), Julio Gonzalez (SGU), Jan Sverre Sandstad (NGU), Elena Savva (RAS).
Uncolored areas correspond to Archean metamorphic rocks and granitoids.
LGB – Lapland Granulite belt, T – Tana belt, LK – Levajok granulite, KT – Korva–Tundra, GR – Gridino eclogite, RW – Rombak Window, CLG – Central Lapland granitoid complex.
Areas with supracrustal units: VA – Vanna, TO – Torsnes, AS – Astridal, AL – Alta, RE – Reppafjord, KK – Kautokeino, KR – Karasjok, KRS – Kiruna–Rensjön–Soppero, MA – Malmberget, VG – Vittangi–Gällivare, HJ – Hietajoki, PE – Peräpohja, KUU – Kuusamo, PS – Posio, KA – Kainuu, KI – Kittilä, KJ – Kuolajarvi, KL – Kalevala, SH – Shombozero, LE – Lehta, ON – Onega, KM – Kumsa, JA – Jangozero, EL – Elmozero, VB – Vetrennyi Belt

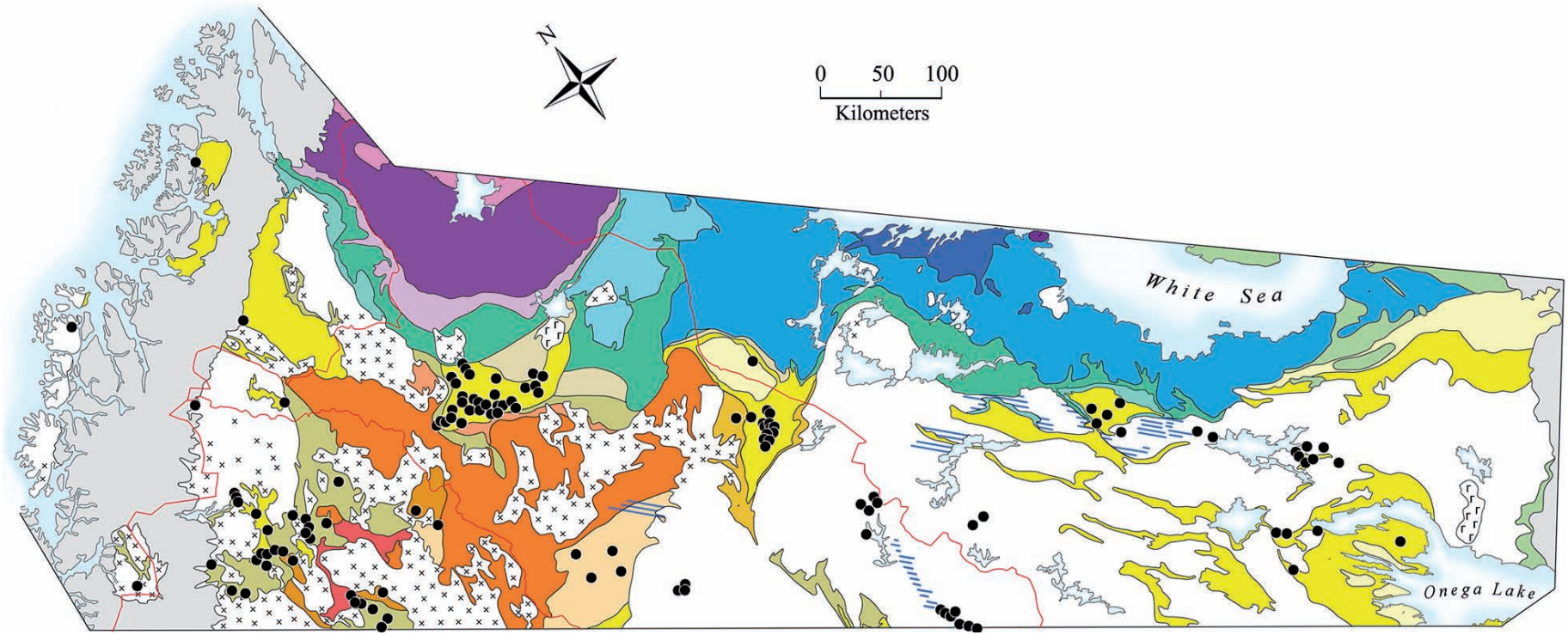

Fig. 5. Distribution of orogenic gold mineralization and its relations with LT–LP metamorphic facies.

Legend as in Fig. 4. Small solid circles mark sites of orogenic gold mineralization. Circles in uncolored areas show mineralization in Archean greenstone belts, as in Fig. 3

The *plagioclase-kyanite-omphacite eclogite subfacies (28)* corresponds to the temperature conditions of the high-amphibolite and granulite facies. The low-T boundary of *subfacies 28* with *subfacies 27* is defined by the disappearance of the zoisite+kyanite+quartz assemblage and appearance of plagioclase in eclogite as a product of the reaction Zo+Ky+Qu+Ab = Pl_{CaNa}.

The low-P boundary of the *plagioclase-kyanite-omphacite subfacies (28)* with amphibolite and granulite facies is well specified in Ca-rich rocks by the appearance of the omphacite+kyanite+garnet paragenesis due to the reaction of plagioclase with hornblende or orthopyroxene: Hb+Pl = Om+Gr+Ky+Qu and Opx+Pl = Gr+Om+Ky+Qu. Eclogite-like clinopyroxene–plagioclase–garnet rocks are also widespread in this transitional zone. In metapelites at the low-P boundary, the kyanite+orthoclase paragenesis of the amphibolite and granulite facies remains stable under eclogite facies conditions, but the granulite orthopyroxene+kyanite paragenesis disappears: Opx_{Mg}+Ky = Gr_{Mg}+Qu. In K-poor Mg-metapelites, talc can appear in the paragenesis with kyanite as a product of the reactions Crd_{Mg} = Ta+Ky+Qu (*subfacies 27* and *28* at the boundary with the amphibolite facies) and Opx_{Mg}+Qu = Ta+Ky (*subfacies 28* at the boundary with the granulite facies).

3. Conditions, setting, and evolution of metamorphism

Typical parageneses of metamorphic facies/subfacies (Fig. 1) formed after various protolith and characterized above are listed in Table 2. The attention is focused on metamorphic facies belonging to the andalusite–sillimanite and kyanite–sillimanite facies series which predominate in the Fennoscandian Shield. The metamorphic conditions are presented with regard to their spatial relations with the major tectonic units of the Fennoscandian Shield (Fig. 2). The maps (Fig. 3, 4) show the prevailing P-T conditions of regional metamorphism of Archean and Proterozoic age. The small scale of Figures 3 and 4 allows us to display only groups of undivided subfacies. Because of this, the maps do not show small relicts of older metamorphism. The color code is used for metamorphic facies series of andalusite-sillimanite and kyanite-sillimanite types as reflecting high and low thermal T/P gradients [Miyashiro, 1961; Hietanen, 1967; Glebovitsky, 1971, 1973; Brown, 2007, 2014]. Intrusive rocks that are either weakly metamorphosed or not metamorphosed at all, and preserve their primary magmatic textures and mineral composition are left colorless. The maps do not show younger overprinting metamorphism related to shear zones of Svecofennian age, because it is not possible to portray it on this scale. Nevertheless, the map of Proterozoic metamorphism (Fig. 4) does show certain areas in Finland and Russia with overprinting metamorphism as zones with colored stripes superimposed on a background color (or uncolored) areas corresponding to regional metamorphism. These high-P and low- to medium-T (rarely high-T) shear zones are widespread over the territory of the Karelian craton and were locally found in the Svecofennian orogen. These shear zones are characterized by high-P metamorphism of the Ky-Sil type (parageneses with kyanite in metapelites and with garnet in metabasites). Also, the maps do not show late retrograde metamorphism related to the exhumation of the metamorphic complexes (assemblages with late andalusite, sillimanite-fibrolite, etc.) and various metasomatic processes in shear zones.

In constructing the maps we made use of data presented in the Map of mineral facies of metamorphic rocks in the Eastern Baltic Shield [Belyaev et al., 1991], Map of metamorphism and transpression tectonics of the Precambrian of Karelia [Volodichev, 2002], and in the Geological map of the Fennoscandian Shield [Koistinen et al., 2001]. For the territory of Norway we also used data published in [Gaal et al., 1978; Barbey et al., 1980; Bernard-Griffiths et al., 1984; Krill, 1985; Marker, 1988, 1991; Marker et al., 1990; Bergh et al., 2010]. For Sweden data were taken from [Idman, 1988; Sawyer, Korneliussen, 1989; Bergman et al., 2001; Käpyaho et al., 2007; Bushmin et al., 2013]. Data on Finland were compiled from [Eskola, 1952; Korsman et al., 1984, 1999; Perttunen et al., 1996; Pajunen, Poutiainen, 1999; Hölttä et al., 2000, 2007, 2012; Hölttä, Paavola, 2000; Laajoki, 2000; Evins, Laajoki, 2001; Räsänen, Vaasjoki, 2001; Mänttäri, Hölttä, 2002; Tuisku et al., 2006; Tuisku, Huhma, 2006; Käpyaho et al., 2007; Kontinen et al., 2007; Kivisaari, 2008; Bushmin et al., 2013]. For the territory of Russia data were published in [Shemyakina, 1983; Baikova et al., 1984; Chekulaev, Baikova, 1984; Lobach-Zhuchenko et al., 1986, 1993, 2000; Belyaev et al., 1990, 1991; Volodichev, 1990, 1994, 1997, 2002; Daly, Bogdanova, 1991; Bibikova et al., 1993, 1995, 1999, 2001a, 2001b, 2004; Frisch et al., 1995; Miller et al., 1995; Astafiev, 1996; Glebovitsky, 1996, 1997, 2005; Glebovitsky et al., 1996, 2000; Sedova et al., 1996; Gerya, 1999; Perchuk et al., 1999, 2000; Miller, 2002; Volodichev et al., 2002, 2004, 2011; Balagansky et al., 2005; Balagansky, Glebovitsky, 2005; Bushmin et al., 2007, 2009, 2013; Mints et al., 2007; Kuleshevich, Lavrov, 2011; Skublov et al., 2011; Lebedeva et al., 2012; Myskova et al., 2012].

Table 2. Typical mineral parageneses of subfacies in various types of metamorphic rocks

Rock type	Paragenesis	Comment
Greenschist facies		
Stilpnomelane-muscovite-chlorite subfacies (1) *(subfacies -1a in And-Sil complexes and subfacies -1b in Ky-Sil complexes)*		
Al-metapelites	Qu+Prl+Mu+Chl	
K-metapelites	Qu+Chl+Mu±Ab	
K-poor metapelites	Qu+Prl+Chl Qu+Stp+Chl±Tc	FeMg-Tc
K-metasandstones	Qu+Ab+Chl+Mu±Stp±Kfs	
Metasandstones	Qu+Ab+Chl+Mu±Ep±(Ank, Cal)	
Metabasites	Qu+Ab+Chl+Ep+Act±(Ank, Cal)	
Muscovite-chlorite-biotite subfacies (2) *(subfacies 2a in And-Sil complexes and subfacies 2b in Ky-Sil complexes)*		
Al-metapelites	Qu+Ctd+Ky(And)+Mu+Chl±Prl	Fe-Ctd
K-metapelites	Qu+Chl+Mu±Ab±Bt	Chl_{0-100}
K-poor metapelites	Qu+Ctd+Chl ±Ky(And) Qu+Stp+Chl±Cum±Tc	Fe-Cum, FeMg-Tc
K-metasandstones	Qu+Ab+Bt+Chl+Mu±Kfs	
Metasandstones	Qu+Ab+Chl+Mu+Bt±(Ank,Cal)±Ep	Chl_{0-100}
Metabasites	Qu+Ab+Act+Chl+Ep±(Ank,Cal)	
Calc-silicates	Cal+Dol+Qu±Ank±Chl±Czo±Scp	
Chlorite-chloritoid-almandine subfacies (3)		
Al-metapelites	Qu+Ctd+ Ky(And)+Chl+Mu Qu+Gr+Ctd+Chl+Mu	Chl_{25-100} Gr_{0-10}
K-metapelites	Qu+Gr+Chl+Mu±Ab(Pl)±Bt	Chl_{25-100}, Gr_{0-10}
K-poor metapelites	Qu+Ctd+Chl±Gr±Ky Qu+Cum+Chl±Gr±Stp	
K-metasandstones	Qu+Bt+Mu±Mi+Ab(Pl)	
Metasandstones	Qu+Bt±Gr+Chl+Mu±Ep+Ab(Pl)	Gr_{0-10}, Chl_{25-100}
Metabasites	Qu+Ab(Pl)+Act+Chl+Ep±Gr ±(Ank,Cal)	Al-Act, Chl_{25-100}
Calc-silicates	Cal+Dol+Qu±Ank±Chl±Czo±Scp	
Amphibolite facies		
Chlorite-chloritoid-staurolite zones 4a and 5a in low-T part of subfacies (4) and (5)		
Al-metapelites	Qu+St+Ctd±Chl+Ky(And)+Mu Qu+Ctd+Gr+Chl± Bt+Mu	Gr_{0-15}, Chl_{40-100}
K-metapelites	Qu+Gr+Bt+Chl+Mu±Pl	Gr_{0-15}, Chl_{40-100}
Mg-metapelites	Qu+Bt+Crd+Chl+Mu (And-Sil complexes)	Mg-Bt, Mg-Crd
K-poor metapelites	Qu+St+Ctd±Gr±Ky(And) Qu+Cum+Chl±Gr	
K-metasandstones	Qu+Pl+Bt+Mu±Kfs±Gr	
Metasandstones	Qu+Pl+Bt+Gr+Chl+Mu±Ep	Gr_{0-15}, Chl_{40-100}
Metabasites	Qu+Pl+Hb+Chl+Ep±Ank,Cal±Gr	Hb blue-green, Chl_{40-100}
Calc-silicates	Cal+Dol+Qu±Hb±Ank±Chl±Czo(Zo)±Scp±(Grs-Adr)	Hb colorless
Andalusite-chlorite-staurolite (4) and kyanite-chlorite-staurolite (5) subfacies		
Al-metapelites	Qu+St+Chl+Ky(And)+Gr+Mu	Chl_{50-100}
K-metapelites	Qu+Bt+Gr+St+Chl+Mu	Gr_{0-20}, Chl_{50-100}
Mg-metapelites	Qu+Bt+Crd+Chl+Mu (And-Sil complexes)	Mg-Bt, Mg-Crd
K-poor metapelites	Qu+St+Gr+Ky(And)±Chl Qu+Cum±Chl±Ant+Gr	
K-metasandstones	Qu+Pl+Bt+Mu±Kfs±Gr	
Metasandstones	Qu+Pl+Bt±Gr±Chl+Mu±Ep	Gr_{0-20}, Chl_{55-100}
Metabasites	Qu+Pl+Hb+Gr ±Czo(Zo) (Ky-Sil complexes)	Hb blue-green, Chl_{50-100}, Gr_{0-20}
	Qu+Pl+Hb±Cum+Chl+Ep±Ank,Cal (And-Sil complexes)	
Calc-silicates	Dol+Qu (or Tr+Cal) ±Hb±Chl+Czo(Zo)±Scp±(Grs-Adr)	Hb colorless

Table 2 continued

Rock type	Paragenesis	Comment
Andalusite-biotite-staurolite (6) and kyanite-biotite-staurolite (8) subfacies		
Al-, K-metapelites	Qu+St+Ky(And)+Bt+Mu Qu+St+Gr+Bt+Mu	Gr_{0-25}
Mg-metapelites	Qu+Bt+Ky+Mu±Crd (Ky-Sil complexes)	Crd_{85-100}, ±Chl_{70-100}
	Qu+Bt+Crd+And+Mu (And-Sil complexes)	Crd_{70-100}, ±Chl_{70-100}
K-poor metapelites	Qu+Gd+Ky+St (Ky-Sil complexes)	
	Qu+St+Crd+Gr+And (And-Sil complexes) Qu+Cum+Gr+Gd	
K-metasandstones	Qu+Pl+Bt+Mu±Kfs±Gr	
Metasandstones	Qu+Pl+Bt+Mu±Gr±Ep	Gr_{0-25}
Metabasites	Qu+Pl+Hb+Gr+Zo (Ky-Sil complexes, *subfacies 8*) Qu+Pl+Hb+Gr	Hb blue-green, Gr_{0-25}, ±Mg-Chl, ±Ep
	Qu+Pl+Hb±Cum (And-Sil complexes) Qu+Pl+Cum	
Calc-silicates	Tr+Cal+Qu (or Cpx) ± Hb±Czo(Zo)±Scp±(Adr-Grs)	Hb colorless, ±Chl, first Cpx (Di)
Sillimanite-biotite-staurolite subfacies (7)		
Al-, K-metapelites	Qu+St+Sil+Gr+Bt+Mu±Pl	Gr_{0-30}
Mg-metapelites	Qu+Bt+Sil+Mu±Crd (Ky-Sil complexes)	±Crd_{80-100}
	Qu+Bt+Crd+Sil+Mu (And-Sil complexes)	Crd_{65-100}
Metabasites	Qu+Pl+Hb+Gr (Ky-Sil complexes, *subfacies 7b*)	
	Qu+Pl+Hb±Cum (And-Sil complexes, *subfacies 7a*) Qu+Pl+Cum	
In other rock types, the parageneses are similar to *subfacies 6* and *8*		
Chlorite-andalusite-garnet-cordierite zone 9a in low-T part of subfacies 9 up to chlorite disappearance		
Al-, K-metapelites	Qu+And+Mu±Chl±Crd±Gr, Qu+Mu+Chl+Bt±Gr	
Mg-metapelites	Qu+And+Crd+Chl+Mu	
K-poor metapelites	Qu+Crd±Gr±Chl+Gd Qu+Cum+Chl+Gd(Ant)±Crd	
K-metasandstones	Qu+Pl+Bt+Mu±Kfs	
Metasandstones	Qu+Pl+ Bt+Chl+Mu±Ep	
Metabasites	Qu+Pl+Hb ±Cum+Chl+Ep	Hb blue-green
Andalusite-biotite-muscovite (9), sillimanite-biotite-muscovite (10), kyanite-biotite-muscovite (11) subfacies		
Al-, K-metapelites	Qu+Ky+Bt+Mu+Gr Qu+And(Sil)+Bt+Mu+Crd±Gr	
Mg-metapelites	Qu+Sil(Ky,And)+Bt+Mu+Crd	
K-poor metapelites	Qu+Gd+Sil+Gr+Crd (Ky-Sil complexes, *subfacies10b*) Qu+Gd+Ky+Gr	
	Qu+Crd+Sil+Gr (And-Sil complexes, *subfacies 10a*) Qu+Ant+And+Crd, Qu+Opx+Cum±Ant±Gr	First Fe-Opx
K-metasandstones	Qu+Pl+Bt+Mu±Gr±Kfs	
Metasandstones	Qu+Pl+Bt+Gr+Mu±Ep	
Metabasites	Qu+Pl+Hb+Gr+Zo (Ky-Sil complexes, *subfacies 11*) Qu+Pl+Hb+Gr (Ky-Sil complexes, *subfacies 10b, 11*) Qu+Pl+Hb±Cum (And-Sil complexes, *subfacies 9, 10a*) Qu+Pl+Cum (And-Sil complexes, *subfacies 9, 10a*)	Hb blue-green
Calc-silicates	Tr+Cal+Qu (or Cpx±Cal±Tr) ±Hb±Czo(Zo)±Scp±(Adr-Grs)	Hb colorless or pale green
Biotite-sillimanite-orthoclase subfacies (14) *(subfacies 14a in And-Sil complexes and subfacies 14b in Ky-Sil complexes)*		
Al-, K-metapelites	Qu+Bt+Sil+Kfs Qu+Bt+Sil+Gr±Kfs Qu+Bt+Sil+Crd±Kfs or Gr	FeMg-Gr
Mg-metapelites	Qu+Bt+Sil+Crd±Kfs	
K-poor metapelites	Qu+Gr+Sil+Gd±Crd (Ky-Sil complexes, *subfacies 14b*)	
	Qu+Opx+Gr±Gd±Cum±Crd	Fe-Opx
K-metasandstones	Qu+Pl+Bt+Kfs±Gr	

End of Table 2

Rock type	Paragenesis	Comment
Metasandstones	Qu+Pl+Bt±Gr	
Metabasites	Qu+Pl+Hb+Gr (Ky-Sil complexes, *subfacies 14b*)	Hb green, brown-green ±Cpx, Opx
	Qu+Pl+Hb±Cum (And-Sil complexes, *subfacies 14a*) Qu+Pl+Cum	
Calc-silicates	Cpx+Cal±Pl±Hb±Dol±Fo±Scp±(Grs-Adr)	
***Biotite-andalusite-orthoclase subfacies* (*12*)**		
Al-, K-metapelites	Qu+Bt+And+Kfs Qu+Bt+And+Crd±Kfs or Gr	
Mg-metapelites	Qu+Bt+Kfs+And+Crd	
K-poor metapelites	Qu+Ant+And+Crd±Gr	
Metabasites	Qu+Pl+Hb±Cum, Qu+Pl+Cum	
In other rock types, the parageneses are similar *to subfacies 14*		
***Biotite-kyanite-orthoclase subfacies* (*15*)**		
Al-, K-metapelites	Qu+Bt+Ky+Gr±Kfs	
Mg-metapelites	Qu+Bt+Ky+Crd±Kfs	
K-poor metapelites	Qu+Gd+Ky+Gr	
Metabasites	Qu+Pl+Hb+Gr+Zo, Qu+Pl+Hb+Gr	± Cpx, Opx
In other rock types, the parageneses are similar to *subfacies 14*		
Granulite facies		
***Biotite-garnet-orthoclase-orthopyroxene subfacies* (*16*)** *(subfacies 16a in And-Sil complexes and subfacies 16b in Ky-Sil complexes)*		
Al-, K-, Mg-metapelites	Qu+Bt+Opx+Kfs±Gr Qu+Bt+Kfs±Gr±Crd Qu+Sil+Kfs±Gr±Crd	FeMg-Opx FeMgAl-Bt
K-poor metapelites	Qu+Opx±Gr±Crd	
Metabasites	Qu+Pl±Hb+Opx+Gr (Ky-Sil complexes, *subfacies 16b*) Qu+Pl±Hb+Cpx+Gr±Opx	Hb brown-green FeMg-Opx
	Qu+Pl±Hb+Cpx±Opx (And-Sil complexes, *subfacies 16a*)	
Calc-silicates	Cpx±Cal±Pl±Hb±Fo±Wo±Grs-Adr	
***Biotite-garnet-sillimanite-orthoclase subfacies* (*17*)**		
Al-, K-, Mg-metapelites	Qu+Bt+Sil+Gr±Kfs or Crd Qu+Bt+Sil+Kfs Qu+Bt+Opx+Kfs±Gr	FeMgAl-Bt FeMg-Opx
K-poor metapelites	Qu+Opx±Gr±Crd	
Metabasites	Qu+Pl±Hb+Cpx+Gr±Opx Qu+Pl±Hb+Opx+Gr	Hb brown-green FeMg-Opx
Calc-silicates	Cpx±Cal±Pl±Hb±Fo±Wo±Grs-Adr	
***Garnet-cordierite-orthoclase-orthopyroxene subfacies* (*19*)** *(subfacies 19a in And-Sil complexes and subfacies 19b in Ky-Sil complexes)*		
Al-, K-, Mg-metapelites	Qu±Bt+Opx+Kfs+Crd±Gr Qu+Bt+Kfs±Crd±Gr Qu+Sil+Kfs±Crd±Gr	Mg-Opx MgAl-Bt
K-poor metapelites	Qu+Opx±Gr±Crd	Mg-Opx
Metabasites	Qu+Pl+Cpx+Gr±Opx (Ky-Sil complexes, *subfacies 19b*) Qu+Pl+Opx+Gr	FeMg-Opx
	Qu+Pl+Cpx±Opx (And-Sil complexes, *subfacies 19a*)	
Calc-silicates	Cpx±Cal±Pl±Hb±Fo±Wo±Grs-Adr	
***Sillimanite-orthopyroxene subfacies* (*20*)**		
Al-, K-, Mg-metapelites	Qu±Bt±Kfs+Sil+Opx±Gr or Crd	MgAl-Bt, Mg-Opx, Mg-Gr, Mg-Crd
K-poor metapelites	Qu+Opx±Gr±Crd	Mg-Crd
Metabasites	Qu+Pl+Cpx+Gr±Opx, Qu+Pl+Opx+Gr	FeMg-Opx, ±Hb brown
Calc-silicates	Cpx±Cal±Pl±Hb±Fo±Wo±Grs-Adr	

Note. Subscript indexes at mineral abbreviations are Mg / (Mg+Fe) mol. %

Sites of orogenic gold mineralization are shown according to [Raw Mineral Base of the Republic of Karelia, 2006; Eilu, 2012].

Archean metamorphism of the Karelian craton and its relict enclaves within the Svecofennian orogen (Fig. 2, 3) corresponds mostly to high T/P gradient conditions of the And-Sil facies series, suggesting high heat flow through the earth's crust at that time. The metamorphic grade of the Archean greenstone belts increases rapidly from their central parts (greenschist facies) toward the margins (low-T to medium-T amphibolite facies). The greenstone belts themselves are metamorphosed at a lower grade than their host TTG gneisses and migmatites, which were metamorphosed to the high-T amphibolite facies and, locally, even to the granulite facies. The Archean greenstone belts can be subdivided into two groups according to their metamorphic grade: (a) belts with predominant metamorphism up to medium-T amphibolite facies and (b) belts with predominant metamorphism to the greenschist facies. The first group is located mostly in the western part of the Karelian craton and seems to be spatially related to areas with granulite facies rocks. The second group is found at a considerable distance from granulites mostly in the east. The metamorphic regime of the Belomorian-Lapland orogen (Fig. 2, 3) was fundamentally different in the Archean and corresponded to the low T/P gradient conditions of the Ky-Sil facies series [Glebovitsky, 1973; Volodichev, 1990]. Evidence of this type of metamorphism is presented by remnants of high-P granulites of the West-Belomorian granulite belt [Glebovitsky, 1997] that are found in Proterozoic amphibolite facies rocks.

The pressure conditions of *Paleoproterozoic metamorphism* differ dramatically between discrete tectonic zones (Fig. 2, 4). During that time two paired metamorphic belts [Brown, 2010] were developed: (1) the Belomorian-Lapland collision orogen with low T/P gradient metamorphism of the Ky-Sil facies series [Glebovitsky, 1973, 1993; Volodichev, 1990; Glebovitsky et al., 1996; Volodichev et al., 2002] and (2) the Svecofennian accretionary orogen with high T/P gradient metamorphism of the And-Sil facies series [Sudovikov et al., 1970; Korsman et al., 1984; Glebovitsky, 1996, 1997; Korsman et al., 1999]. Also, Svecofennian low- to medium-T (occasionally high-T) high-P metamorphism of the Ky-Sil facies series locally overprinted Archean and Paleoproterozoic metamorphism along shear zones in the Karelian craton and, to a lesser extent, Paleoproterozoic metamorphism at the margin of the Svecofennian orogen.

The Belomorian-Lapland orogen, including the Lapland Granulite belt, is characterized by inverted metamorphic zoning, which is typical of collisional orogens. In the Svecofennian orogen, metamorphic zoning is closely connected with granitoid magmatism as is typical of accretionary orogens. Similar to the Archean greenstone belts, some of the Paleoproterozoic rift-related belts in the Karelian craton and Svecofennian orogen exhibit an increase in the metamorphic grade toward the margins.

The metamorphic area in question encompasses a part of the Sveco-Karelian zone (Fig. 2), which belongs to the Svecofennian accretionary orogen and hosts numerous sites with orogenic gold mineralization (Fig. 5). This zone is a reworked Archean continental margin recycled by Svecofennian accretionary processes in the Paleoproterozoic. The Paleoproterozoic high T/P gradient metamorphism of the And-Sil type and synmetamorphic or subsequent LT-LP hydrothermal-metasomatic processes that produced Au mineralization in shear zones, as is typical of the Svecofennian orogen, suggest fundamental controls by deep-seated accretionary processes along the Archean continental margin. This type of relationships results in a spatial and genetic connection between orogenic gold mineralization and areas of high T/P metamorphism of the And-Sil type. These facts and considerations suggest certain specifics of the mantle plume evolution, the derivation and emplacement of magmatic melts at various crustal depths, and deep circulation of gold-bearing fluids, as is typical of continental margins of accretion type [e. g. Hronsky et al., 2012]. Relations between orogenic gold mineralization (Fig. 5) and LT-LP metamorphism and metasomatism in shear zones were controlled by transport properties of fluids and by P-T conditions favourable for mechanisms of gold precipitation from fluids. Consequently, the most promising exploration targets for orogenic gold deposits are areas of low-P And-type greenschist and low amphibolite facies [Bushmin, 1989, 1996; Bushmin et al., 2013]. Such areas are present in the Peräpohja belt, Kuusamo belt, and in the Kittilä area in Finland, in the Norrbotten area in Sweden, in the Kautokeino, Repparfjord, and Alta areas in Norway, in the Kuolajarvi area in Russia.

In contrast to the Sveco-Karelian zone of the Svecofennian orogen, the Karelian craton hosts not many sites with Archean and Proterozoic orogenic gold mineralization in Archean greenstone belts and Paleoproterozoic rift-related belts (Fig. 5). Among them there are only few sites with Archean orogenic gold in Finland (no Archean orogenic gold has yet been found in the Russian part) due to the following reasons. The grade of Archean metamorphism at most of the preserved Archean greenstone belts with shear zones is higher than the parameters of the greenschist facies. This

means that the productive upper LT-LP parts of Archean shear zones were eroded and are not exposed any more at the surface. We suppose that this could be the reason for the scarce sites of economic Au mineralization in Archean shear zones of the Karelian craton.

Furthermore, Svecofennian high-P metamorphic-metasomatic processes superimposed on Archean and Paleoproterozoic metamorphic rocks along shear zones in greenstone and rift-related belts could play the role of an additional negative factor for gold mineralization. Yet, fluid-permeable shear zones accompanied by LT-LP metasomatism with gold mineralization were formed again at late-Svecofennian time [Glebovitsky et al., 2014]. The North Onega region in the Russian part of the Karelian craton is an example of a promising area for orogenic gold deposits [e. g. Borozdin et al., 2014] of late-Svecofennian age.

This investigation was financially supported by the Russian Foundation for Basic Research (S. A. Bushmin, Project 13-05-00393) and was carried out under the international Project «Fennoscandian Gold Transect» (headed by Raimo Lahtinnen, GTK, Espoo, Finland and Nikolai Philippov, State Company Mineral, St. Petersburg, Russia).

We thank Julio Gonzalez, Jan Sverre Sandstad, Dmitry V. Dolivo-Dobrovolsky, and Vasiliy I. Ivashenko for valuable discussions of scientific problems outlined in the paper. The authors acknowledge the helpful review comments and suggestions of Pekka Tuisku and Pentti Hölttä. The authors also thank Pentti Hölttä for supplying data on metamorphic rocks of Finland. Comments made by two anonymous reviewers substantially improved the paper. We are grateful to Galina P. Pleskach for drafting the figures.

References

Aranovich L. Ya., Berman R. G. Optimized standard state and solution properties of minerals: II. Comparisons, predictions, and applications. *Contrib. Mineral. Petrol*. 1996. Vol. 126. P. 25–37.

Ashley K. T., Law R. D. Modeling prograde TiO_2 activity and its significance for Ti-in-quartz thermobarometry of pelitic metamorphic rocks. *Contrib Mineral Petrol*. 2015. 169:23.

Astafiev B. Y. Metasomatites of the metamorphic rocks of the Karelian megablock. 1996. PhD. Thesis. Leningrad. 21 p. (in Russian).

Baikova V. S., Lobach-Zhuchenko S. B., Levchenkov O. A., Cheekulaev V. P., Shuleshko I. K., Yakovleva S. Z. New data on the geological position and age of granulites of Karelia. *Doklady AS USSR*. 1984. Vol. 277, no. 2. P. 442–444 (in Russian).

Balagansky V. V., Glebovitsky V. A. Lapland granulite belt and complimentary structures. In Glebovitsky V. A. (ed.). Early Precambriam of the Baltic Shield. Leningrad: Nauka, 2005. P. 124–175 (in Russian).

Balagansky V. V., Kaulina T. V., Kislitsin R. V. Kolvitsa mélange and Umba terrain as a new type of Paleoproterozoic structures in northeast of the Baltic shield. In: Petrography of the 21st century. Abstracts. Apatity. 2005. Vol. 3. P. 39–41 (in Russian).

Barbey P., Convert J., Martin H., Capdevila R., Hameurt J. Relationships between granite-gneiss terrains, greenstone belts and granulite belts in the Archean crust of Lapland (Fennoscandia). *Geol. Rundsch. Bd*. 1980. Vol. 69. P. 648–658.

Belyaev O. A., Bushmin S. A., Volodichev O. I., Glebovitsky V. A., Klein B. M., Kuleshevich L. V., Petrov V. P., Severin V. V. Metamorphic facies of the Eastern part of the Baltic Shield. Leningrad: Nauka, 1990. 141 p. (in Russian).

Belyaev O. A., Bushmin S. A., Voinov A. S., Volodichev O. I., Glebovitsky V. A. et al. Map of mineral facies of metamorphic rocks in the eastern Baltic Shield in the scale 1:1 500 000 (ed. V. A. Glebovitsky). St. Petersburg: VSEGEI, IPGG RAS, 1991.

Bergh S. G., Kullerud K., Armitage P. E. B., Zwaan K. B., Corfu F., Ravna E. J. K., Myhre P. I. Neoarchaean to Svecofennian tectono-magmatic evolution of the West Troms Basement Complex, North Norway. *Norwegian Journal of Geology*. 2010. Vol. 90. P. 21–48.

Bergman S., Kübler L., Martinsson O. Description of regionalgeological and geophysical maps of northern Norrbotten County (east of the Caledonian orogen). *Sveriges geologiska undersökning.* 2001. Ba 56. 110 p.

Berman R. G. Thermobarometry using multiequilibrium calculations: a new technique with petrologic applications. *Canadian Miner*. 1991. Vol. 29. P. 833–855.

Berman R. G., Easton R. M., Nadeau L. A. New tectonometamorphic map of the Canadian shield: Introduction. *Canadian Miner.* 2000. Vol. 38. P. 277–285.

Bernard-Griffits J., Peucat J. J., Postaire B., Vidal Ph., Convert J., Moreau B. Isotopic date (U-Pb, Rb-Sr, Pb-Pb and Sm-Nd) on mafic granulites from Finnish Lapland. *Precambrian Res*. 1984. Vol. 23. P. 325–348.

Bibikova E. V., Sheld T., Bogdanova S. V. et al. Geochronology of belomorides: interpretation of polystage geological history. *Geochemistry*. 1993. No. 10. P. 1393–1411 (in Russian).

Bibikova E. V., Slabunov A. I., Kirnozova T. I. et al. U-Pb age of zircons from the rocks of the Keret' granite-greenstone system in the joint zone of Karelian and Belomorian structures of the Baltic shield. *Doklady RAS*. 1995. Vol. 343, no. 4. P. 517–521 (in Russian).

Bibikova E. V., Slabunov A. I., Bogdanova S. V., Sheld T. Tectono-thermal evolution of the Earth's crust in the Karelian and Belomorian provinces of the Baltic shield in the early Precambrian by U-Pb isotope data for titanites and retiles. *Geochemistry*. 1999. No. 8. P. 1–15 (in Russian).

Bibikova E. V., Clyson S., Glebovitsky V. A. et al. Isotope dating of the Svecofennian stage of Belomo-

rian belt transformation (Baltic shield). *Geochemistry*. 2001a. No. 10. P. 1023–1026 (in Russian).

Bibikova E., Skiöld T., Bogdanova S., Gorbachtschev R., Slabunov A. Titanite-rutile thermochronometry acrossthe boundary between the Archean Craton in Karelia and the Belomorian Mobile Belt, eastern Baltic Shield. *Precambrian Res.* 2001b. Vol. 105. P. 315–330.

Bibikova E. V., Bogdanova S. V., Glebovitsky V. A., Clyson S., Sheld T. Stages of evolution of the Belomorian mobile belt by U-Pb zircon geochronology (NORDSIM). *Petrology*. 2004. Vol. 12, no. 3. P. 227–244 (in Russian).

Borozdin A. P., Polekhovskii Yu. S., Bushmin S. A., Glebovitskii V. A., Belyatskii B. V., Savva E. V. Age of metasomatism and ore formation in the Srednyaya Padma vanadium–precious metals–uranium deposit (Karelia, Baltic Shield). *Doklady Earth Sciences*. 2014. Vol. 454. Part 1. P. 68–71.

Brown M. Metamorphism, Plate Tectonics, and the Supercontinent Cycle. *Earth Science Frontiers*, 2007. Vol. 14 (1). P. 1–18.

Brown M. Paired metamorphic belts revisited. *Gondwana Research*. 2010. Vol. 18. P. 46–59.

Brown M. The contribution of metamorphic petrology to understanding lithosphere evolution and geodynamics. *Geoscience Frontiers*. 2014. Vol. 5, no. 4. P. 553–569.

Bucher K., Frey M. Petrogenesis of metamorphic rocks. Springer. 2002. 341 p.

Bushmin S. A., Glebovitsky V. A. Scheme of mineral facies of metamorphic rocks. *Geology of Ore Deposits*. 2008. Vol. 50, no. 8. P. 659–669.

Bushmin S. A. Facies, facies series of metasomatism and ore speciation of metamorphic belts / In: Zharikov V. A. (ed.) Precambrian metasomatic rocks and their ore-bearing potential. Moscow: Akad. Nauk USSR, 1989. P. 46–64 (in Russian).

Bushmin S. A. Metasomatic rocks in the zones of regional metamorphism. In: Geologic research of metamorphic and metasomatic complexes. St. Petersburg: VSEGEI, 1996. P. 84–125 (in Russian).

Bushmin S. A., Dolivo-Dobrovolsky D. V., Lebedeva Yu. M. Infiltration metasomatism under conditions of granulite facies of high pressure (on the example of orthopyroxene-sillimanite rocks in the shear zones of the Lapland granulite belt). *Doklady Earth Sciences*. 2007. Vol. 412, no. 3. P. 383–387.

Bushmin S. A., Glebovitskii V. A., Savva E. V., Lokhov K. I., Presnyakov S. L., Lebedeva Yu. M., Sergeev S. A. The age of HP metasomatism in shear zones during collision related metamorphism in the Lapland Granulite Belt: The U/Pb SHRIMP II dates on zircons from sillimanite-hypersthene rocks of the Porya Guba nappe. *Doklady Earth Sciences*. 2009. Vol. 429, no. 8. P. 1342–1345.

Bushmin S., Gonzalez J., Hölttä P., Sandstad J. S., Savva E. Metamorphism within the Fennoscandian Gold Transect (FENGOT) area of Fennoscandian Shield. In: Gold of the Fennoscandian Shield (Ed. A. I. Golubev). Proceedings of the international conference. Petrozavodsk: KarRC RAS, 2013. P. 19–21.

Chekulaev V. P., Baikova V. S. Granulite associations of grey gneisses of Western Karelia. In: Natural associations of Archean grey gneisses (geology and petrology). Leningrad: Nauka, 1984. P. 141–150 (in Russian).

Daly S., Bogdanova S. Timing of the metamorphism in the Lapland granulite belt, Finland. *Research Terrae*. 1991. Ser. A. No. 5, 11.

Dobretsov N. L., Reverdatto V. V., Sobolev V. S., Sobolev N. V., Khlestov V. V. Metamorphic facies. Moscow: Nauka, Nedra, 1970. 432 p. (in Russian).

Dobretsov N. L., Sobolev V. S., Khlestov V. V. Facies of moderate-pressure regional metamorphism. Moscow: Nedra, 1972. 288 p. (in Russian).

Dobretsov N. L., Sobolev V. S., Sobolev N. V., Khlestov V. V. Facies of high-pressure regional metamorphism. Moscow: Nedra, 1974. 328 p. (in Russian).

Eilu P. (ed.) Mineral deposits and metallogeny of Fennoscandia. Geological Survey of Finland. Special Paper. 2012. No. 53. 401 p.

Eskola P. The mineral facies of rocks. *Norsk. Geol. Tidsskr*. 1920. Vol. 6. P. 143–194.

Eskola P. On the Granulites of Lapland. *Amer. J. Sci.* 1952. Vol. 5. P. 133–171.

Evins P. M., Laajoki K. Age of the Tokkalehto metagabbro and its significance to the lithostratigraphy of the early Proterozoic Kuusamo supracrustal belt, northern Finland. *Bulletin of the Geological Society of Finland*. 2001. Vol. 73. Parts 1–2. P. 5–15.

Frisch T., Jackson G. D., Glebovitsky V. A., Efimov M. M., Bogdanov M. N., Perrish P. P. Zircon U-Pb geochronology of the Kolvitsa gabbro-anorthosite complex, southern part of the Kola peninsular, Russia. *Petrology*. 1995. Vol. 3, no. 3. P. 248–254 (in Russian).

Fyfe W. S., Turner F. J., Verhoogen J. Metamorphic reactions and metamorphic facies. Moscow: Inostrannaya Literatura, 1962. 414 p. (in Russian).

Gaál G., Mikkola A., Söderholm B. Evolution of the Archean crust in Finland. *Precambrian Res*. 1978. Vol. 6, no. 2. P. 199–215.

Gerya T. V. P-T trends and the model of Precambrian granulite complexes formation. Dr. Sci. Thesis. Moscow, 1999. 36 p. (in Russian).

Glebovitsky V. A. The metamorphic facial series and the evolution of metamorphic belts. In.: The metamorphic belts of the USSR. Leningrad: Nauka, 1971. P. 269–291 (in Russian).

Glebovitsky V. A. Problems of evolution of metamorphic processes in mobile regions. Leningrad: Nauka, 1973. 128 p. (in Russian).

Glebovitsky V. A. Mineral facies as criteria for evaluation of P-T parameters of metamorphism. In: Thermo- and barometry of metamorphic rocks. Leningrad: Nauka, 1977. P. 5–39 (in Russian).

Glebovitsky V. A. Tectonics and regional metamorphism of the early Precambrian of the eastern part of the Baltic shield. *Regional geology and metallogeny*. 1993. Vol. 1. P. 7–24 (in Russian).

Glebovitsky V. A. Geological and physical-chemical relationship of metamorphism and tectonics in the early Precambrian. *Geotectonics*. 1996. Vol. 5. P. 27–42 (in Russian).

Glebovitsky V. A., Miller Y. V., Drugova G. M., Milkevich R. I., Vrevskii A. B. Structure and metamorphism of the Belomorian-Lapland collision zone. *Geotectonics*. 1996. Vol. 1. P. 63–75 (in Russian).

Glebovitsky V. A. The early Precambrian of Russia. Harwood. Acad. Publ. 1997. 261 p.

Glebovitsky V. A., Zinger T. F., Belyatsky B. V. On the age of granulites of the West-Belomorian belt and nappe formation within it. *Doklady RAS*. 2000. Vol. 371. P. 163–166 (in Russian).

Glebovitsky V. A. (ed.) Early Precambrian of the Baltic Shield. St. Petersburg: Nauka, 2005. 711 p. (in Russian).

Glebovitsky V. A., Bushmin S. A., Belyatsky B. V., Bogomolov E. S., Borozdin A. P., Savva E. V., Lebedeva Yu. M. Rb–Sr Age of metasomatism and ore formation in the low-temperature shear zones of the Karelian craton, Baltic Shield. *Petrology*. 2014. Vol. 22, no. 2. P. 184–204 (in Russian).

Groves D. I., Goldfarb R. J., Gebre-Mariam M., Hagemann S. G., Robert F. Orogenic gold deposits: A proposed classification in the context of their crustal distribution and relationship to other gold deposit types. *Ore Geology Reviews*. 1998. Vol. 13. P. 7–27.

Hietanen A. On the facies serirs in various types of metamorphism. *J. Geol*. 1967. Vol. 75, no. 2. P. 187–214.

Holdaway M. J. Stability of andalusite and the aluminium silicate phase diagram. *Amer. J. Sci*. 1971. Vol. 271, no. 2. P. 97–131.

Hölttä P., Paavola J. P-T-t development of Archean granulites in Varpaisjärvi, Central Finland. I. Effects of multiple metamorphism on the reaction history of mafic rocks. *Lithos.* 2000. Vol. 50. P. 97–120.

Hölttä P., Huhm H., Mänttäri I., Paavola J. P-T-t development of Archean granulites in Varpaisjärvi, Central Finland. II. Dating of high-grade metamorphism with the U-Pb and Sm-Nd methods. *Lithos*. 2000. Vol. 50. P. 121–136.

Hölttä P., Vaisanen M., Vaananen J., Manninen T. Paleoproterozoic metamorphism and deformation in Central Finish Lapland. In: Gold in the Central Lapland Greenstone Belt, Finland. Geological Survey of Finland. Special paper. 2007. Vol. 44. P. 9–44.

Hölttä P., Heilimo E., Huhma H., Juopperi H., Kontinen A., Konnunaho H., Lauri L., Mikkola P., Paavola J., Sorjonen-Ward P. Archean complexes of the Karelia Province in Finland. Geological Survey of Finland. Special Paper. 2012. Vol. 54. P. 9–20.

Hronsky J. M. A., Groves D. I., Loucks R. R., Begg G. C. A unified model for gold mineralisation in accretionary orogens and implications for regional-scale exploration targeting methods. *Mineralium Deposita*. 2012. Vol. 47. P. 339–358.

Idman H. Pre-Quarternary rocks, Sheet-1832-Ropi, Geological map of Finland 1:100 000. Geological Survey of Finland. 1988.

Käpyaho A., Hölttä P., Whitehouse M. U-Pb zircon geochronology of selected Neoarchean migmatites in eastern Finland. *Bulletin of Geological Survey of Finland*. 2007. Vol. 79, no. 1. P. 95–115.

Kivisaari T. Tuntsan metasedimenttivyöhykkeen matamorfoosi. (Ph. D. Thesis). University of Helsinki. 2008. 53 p. (in Finnish).

Koistinen T., Stephens M. B., Bogatchev V., Nordgulen Ø., Wennerström M., Korhonen J. (Comps.). Geological map of the Fennoscandian Shield 1:2 000 000. Espoo; Trondheim; Uppsala; Moscow. 2001.

Kontinen A., Käpyaho A., Huhma H., Karhu J., Matukov D. I., Larionov A., Sergeev S. A. Nurmes paragneisses in eastern Finland, Karelian craton: provenance, tectonic setting and implications for Neoarchean craton correlation. *Precambrian Res*. 2007. Vol. 152. P. 119–148.

Korikovsky S. P. Metamorphic facies of metapelites. Moscow: Nauka, 1979. 213 p. (in Russian).

Korikovsky S. P. Prograde transformations of gabbro-norites during eclogitization in the temperature range 600–700 °C. *Russian Geology and Geophysics*. 2005. Vol. 46, no. 12. P. 1352–1366 (in Russian).

Korikovsky S. P. Prograde transformations of medium-pressure amphibolites during their eclogitization. *Petrology*. 2009. Vol. 17, no. 4. P. 315–330.

Korikovsky S. P. Metamorphic transformations of metapelites, gneisses and granitoids under the conditions of eclogite facies. In: Modern problems of magmatism and metamorphism. 2012. Vol. 1. P. 291–294 (in Russian).

Korikovsky S. P. Mirčovski V., Zakariadze G. S. Metamorphic evolution and the composition of the protolith of plagioclase-bearing eclogite-amphibolites of the Buchim block of the Serbo–Macedonian Massif, Macedonia. *Petrology*. 1997. Vol. 5, no. 6. P. 534–549.

Korikovsky S. P., Somin M. L., Korsakov S. G. High-pressure symplectitic garnet–clinopyroxene–margarite–muscovite–clinozoisite amphibolites of the Dakhov Block, Northern Caucasus: genesis and composition of reaction textures. *Doklady Earth Sciences*. 2004. Vol. 397A, no. 6. P. 778–782.

Korikovsky S. P. Zakariadze G. S., Kolcheva K., Zhelyazkova-Panaiotova M. D., Solov'eva N. V. Albite–epidote–hornblende-bearing eclogite–amphibolites from the Belorechensk Uplift of the Rhodope Massif: Phase equilibria and P–T parameters. *Doklady Earth Sciences*. 1998a. Vol. 359A, no. 3. P. 360–363.

Korikovsky S. P., Zakariadze G. S., Kolcheva K., Zhelyazkova-Panaiotova M. D., Solov'eva N. V. Kataphorite eclogites of the Madan Tectonic Unit of the Crystalline Basement of the Eastern Rhodope. *Doklady Earth Sciences*. 1998b. Vol. 359A, no. 3. P. 372–375.

Korsman K., Hölttä P., Hautala T., Wasenius P. Metamorphism as an indicator of evolution and structure of the crust in eastern Finland. Geological Survey of Finland. 1984. Bulletin 328. 40 p.

Korsman K., Korja T., Papunen M., Virransalo P., GGT/SVEKA Working group. The GGT/SVEKA Transect: Structure and evolution of the continental crust in the Paleoproterozoic Svecofennian orogeny in Finland. *Intern. Geol. Rev*. 1999. Vol. 41. P. 287–333.

Kozlovskii V. M., Aranovich L. Ya., Frishman N. I. Prograde transformations of amphibolites into eclogites and eclogite-like rocks in the low-pressure field of the eclogite facies (by the example of the Belomorian Mobile Belt). *Russian Geology and Geophysics*. 2015. Vol. 56. P. 689–708.

Krill A. G. Svecokarelian thrusting with thermal inversion in the Karasjok-Levajok area of the northern Baltic Shield. *Nor. Geol. Unders*. 1985. Vol. 403. P. 89–101.

Kuleshevich L. V., Lavrov O. B. New data on the mineralogy of Karelia's gold units. In: Geology of Karelia

from the Archaen to the present. Petrozavodsk: KarRC RAS. 2011. P. 149–160.

Laajoki K. The Himmerkinlahti member: an indicator of Intra-Karelian erosion within the early Proterozoic Kuusamo belt, Posio, Northern Finland. *Bulletin of the Geological Society of Finland*. 2000. Vol. 72. Parts 1–2. P. 71–85.

Lebedeva Yu. M., Bushmin S. A., Glebovitskii V. A. Thermodynamic conditions of metasomatism in high-temperature and high-pressure shear zones (Kandalaksha–Umba Zone, Kola Peninsula). *Doklady Earth Sciences.* 2012. Vol. 445. Part 1. P. 874–878.

Lobach-Zhuchenko S. B., Chekulaev V. P., Arestova N. A., Levsky L. K., Kovalenko A. V. Archean terrains of Karelia: their geological and isotope-geochemical grounds. *Geotectonics*. 2000. Vol. 6. P. 26–42 (In Russian).

Lobach-Zhuchenko S. B., Bibikova E. V., Drugov G. M. et al. Geochronology and petrology of the rocks of the magmatic complex of the Tupaya Guba area. *Petrology*. 1993. Vol. 1, no. 6. P. 657–677 (in Russian).

Lobach-Zhuchenko S. B., Levchenkov O. A., Chekulaev V. P., Krylov I. N. Geological evolution of the Karelian granite-greenstone terrain. *Precambrian Res*. 1986. Vol. 33. P. 45–65.

Mahar E. M., Baker J. M., Powell R. et al. The effect of Mn on mineral stability in metapelites. *J. Metam. Geol*. 1997. Vol. 15, no. 2. P. 223–238.

Mänttäri I., Hölttä P. U-Pb dating of zircons and monazites from Archean granulites in Varpaisjärvi, Central Finland: Evidence for multiple metamorphism and Neoarchean terrane accretion. *Precambrian Res*. 2002. Vol. 118. P. 101–131.

Marker M. Early Proterozoic thrusting of the Lapland granulite belt and its geotectonic evolution, northern Baltic Shield. *Geol. Foren. Stockh. Forth*. 1988. Vol. 11. P. 405–411.

Marker M., Henkel H., Lee M. K. Combined gravity and magnetic modelling of the Tanaelv and Lapland granulite belts, Polar profile, Northern Baltic Shield. In.: The European Geotraverse: integrative studies. European science foundation. 1990. P. 67–76.

Marker M. The Lapland Granulite Belt. Res. Terrae. 1991. Ser. A. No. 6. P. 40–66.

Miller Y. V., Milkevich R. I. Nappe-thrust structure of the Belomorian zone and its relation to the Karelian granite-greenstone region. *Geotectonics*. 1995. Vol. 6. P. 359–370 (in Russian).

Miller Y. V. Tectonics in the junction area between the Belomorian mobile belt and the Karelian craton. *Geotectonika*. 2002. Vol. 4. P. 14–28 (in Russian).

Mints M. V., Kaulina T. F., Konilov A. N., Krotov A. V., Stupak V. M. The thermal and geodynamic evolution of the Lapland granulite belt: Implications for the thermal structure of the lower crust during granulite-facies metamorphism. *Gondwana Research*. 2007. Vol. 12. P. 252–267.

Miyashiro A. Evolution of metamorphic belts. *J. Petrol*., 1961. Vol. 2, no. 3. P. 277–311.

Myskova T. A., Ivanov N. M., Korsakova M. A., Milkevich P. I., Presnyakov S. L., Berezhnaya N. G. Composition and age of volcanites of the Vermas unit of Sariolian, North Karelia. *Stratigraphy. Geological Correlation*. 2012. Vol. 20, no. 1. P. 3–17 (in Russian).

Pajunen M., Poutiainen M. Paleoproterozoic prograde metasomatic-metamorphic overprint zones in Archaean tonalitic gneisses. Eastern Finland. *Bulletin of the Geological Society of Finland*. 1999. Vol. 71, no. I. P. 73–132.

Powell R., Holland T. J. B., Worley B. Calculating phase diagrams involving solid solutions via non-linear equations, with examples using THERMOCALC. *J. Metam. Geol.* 1998. No. 16. P. 577–588.

Powell R., Holland T. J. B. On thermobarometry. *J. Metam. Geol*. 2008. No. 26. P. 155–179.

Räsänen J., Vaasjoki M. The U-Pb age of felsic gneiss in the Kuusamo schist area: reappraisal of local lithostratigraphy and possible regional correlations. In: Radiometric age determinations from Finnish Lapland and their bearing on the timing of Precambrian volcano-sedimentary sequences. Geological Survey of Finland. 2001. Special Paper 33. P. 143–152.

Raw Mineral Base of the Republic of Karelia. Vol. 1. (Eds.: Mikhailov V. P., Aminov V. N). Petrozavodsk. 2006. 278 p. (in Russian).

Perchuk L. L., Krotov A. V., Gerya T. V. Petrology of amphibolites of the Tana belt and granulites of the Lapland complex. *Petrology*. 1999. Vol. 7, no. 4. P. 356–381 (in Russian).

Perchuk L. L., Gerya T. V., Van Reenen D. D., Smit C. A., Krotov A. V. P-T paths and tectonic evolution of shear zones separating high-grade terrains from cratons: examples from Kola Peninsula (Russia) and Limpopo Region (South Africa). *Mineral. Petrol*. 2000. Vol. 69. P. 109–142.

Perttunen V., Hansky E., Vaananen J., Eilu P., Lappalainen M. Rovaniemen kartta-allueen kalliopera. Geological Survey of Finland, Espoo, 1996. P. 1–63.

Sawyer E. W., Korneliussen A. The geochemistry of lower Proterozoic siliciclastic turbidites from the Rombak Window: implications for paleogeography and tectonic settings. *Nor. geol. under*. 1989. Bull. 415. P. 23–38.

Sedova I. S., Glebovitsky V. A., Semenov A. P. Evolution of metamorphism of late Archean periond in the Tupaya Guba area of Lake Kovdozero, northwest Belomorie. *Petrology*. 1996. Vol. 4, no. 2. P. 150–170 (in Russian).

Shemyakina N. M. Geochemistry of regional low-temperature metasomatites of the eastern part of the Baltic Shield. PhD Thesis. Leningrad: VSEGEI, 1983. 20 p. (in Russian).

Skublov S. G., Astafiev B. Yu., Marin Yu. B., Berezin A. V., Melnik A. E., Presnyakov S. L. New data of the age of eclogites of the Belomorian mobile belt in Gridino area. *Doklady RAS*. 2011. Vol. 439, no. 6. P. 795–802 (in Russian).

Spear F. S. Metamorphic Phase Equilibria and Pressure-Temperature-Time Paths. Mineralogical Society of America, Washington, D. C., 1993. 799 p.

Sudovikov N. G., Glebovitsky V. A., Sergeev A. S. Geological evolution of deep zones of mobile belts (North Ladoga). Leningrad. 1970. 227 p. (in Russian).

Tinkham D. K., Zuluaga C. A., Stowell H. H. Metapelite phase equilibria modeling in MnNCKFMASH: The effect of variable Al_2O_3 and MgO/(MgO + FeO) on mineral stability. *Geol. Materials Res*. 2001. Vol. 3, no. 1. P. 1–42.

Tuisku P., Huhma H. Evolution of migmatitic granulite complexes: implications from Lapland Granulite Belt. Part 2: Isotopic dating. Geological Survey of Finland. 2006. Bulletin 78. P. 143–175.

Tuisku P., Mikkola P., Huhma H. Evolution of migmatitic granulite complexes: implications from Lapland Granulite Belt, Part I: Metamorphic geology. Geological Survey of Finland. 2006. Bulletin 78. P. 71–105.

Volodichev O. I. Belomorian complex of Karelia (geology and petrology). Leningrad: Nauka, 1990. 245 p. (in Russian).

Volodichev O. I. Amphibole – indicator of metamorphism of Lopian greenstone rocks. In: Mineralogy of magmatic and metamorphic rocks of the Precambrian in Karelia. Petrozavodsk: KarRC RAS, 1994. P. 105–117 (in Russian).

Volodichev O. I. Geologic-petrological features of the subduction stage of the Belomorian collision structure development in the upper Archean. In: Belomorian Mobile belt (geology, geodynamics, geochronology). Absracts. Petrozavodsk: KarRC RAS, 1997. P. 23–24 (in Russian).

Volodichev O. I. Map of metamorphism and transpressive tectonics of the Precambrian of Karelia in the 1:1 000 000 scale. Report: Endogenic regimes of metamorphism in different geodynamic conditions of Precambrian of Karelia (authors: Volodichev O. I., Kuleshevich L. V., Kuzenko T. I.). Fondy IG KarRC RAS. Petrozavodsk. 2002. 185 p. (in Russian).

Volodichev O. I., Korol N. E., Kuzenko T. I., Sibelev O. S. Metamorphism of Early Precambrian complexes in the Eastern Fennoscandian shield. In: Geology of Karelia from the Archaen to the present. Petrozavodsk: KarRC RAS, 2011. P. 49–55 (in Russian).

Volodichev O. I., Kuleshevich L. V., Kuzenko T. I. Endogenic regimes of metamorphism in different geodynamic conditions of the Precambrian of Karelia. Fondy IG KarRC RAS. Petrozavodsk. 2002. 185 p. (in Russian).

Volodichev O. I., Slabunov A. I., Bibikova E. V. et al. Archean eclogites of the Belomorian mobile belt (Baltic shield). *Petrology*. 2004. Vol. 6. P. 609–631.

White R. W., Powell R., Holland T. J. B., Worley B. A. The effect of TiO_2 and Fe_2O_3 on metapelitic assemblages at greenschist and amphibolite facies conditions: Mineral equilibria calculations in the system K_2O–FeO–MgO–Al_2O_3–SiO_2–H_2–Fe_2O_3. *J. Metam. Geol*. 2000. Vol. 18, no. 5. P. 497–511.

Winkler H. D. F. Petrogenesis of metamorphic rocks. Springer-Verlag. 1976. 334 p.

СВЕДЕНИЯ ОБ АВТОРАХ:

Бушмин Сергей Алексеевич
старший научный сотрудник, к. г.-м. н., доцент
Институт геологии и геохронологии докембрия РАН
наб. Макарова 2, Санкт-Петербург, Россия, 199034
эл. почта: s.a.bushmin@ipgg.ru
тел.: +79217561362; +7 (812) 3284701

Глебовицкий Виктор Андреевич
советник РАН, чл.-корр. РАН, д. г.-м. н., проф.
Институт геологии и геохронологии докембрия РАН
наб. Макарова 2, Санкт-Петербург, Россия, 199034
тел.: +7 (812) 3284701

CONTRIBUTORS:

Bushmin, Sergey
Institute of Precambrian Geology and Geochronology RAS
2 Nab. Makarova, 199034 St. Petersburg, Russia
e-mail: s.a.bushmin@ipgg.ru
tel.: +79217561362; +7 (812) 3284701

Glebovitsky, Viktor
Institute of Precambrian Geology and Geochronology RAS
2 Nab. Makarova, 199034 St. Petersburg, Russia
tel.: +7 (812) 3284701